

A posteriori discontinuous Galerkin error estimator for linear elasticity

Robert E. Bird, William M. Coombs, Stefano Giani*

Department of Engineering, Durham University, South Road, Durham DH1 3LE, UK

ARTICLE INFO

MSC:
35J57
65N30
65N50
65N15

Keywords:

Discontinuous Galerkin
Error estimator
Linear elasticity

ABSTRACT

This paper presents for the first time the derivation of an hp a posteriori error estimator for the symmetric interior penalty discontinuous Galerkin finite element method for linear elastic analysis. Any combination of Neumann and Dirichlet boundary conditions are admissible in the formulation, including applying Neumann and Dirichlet on different components on the same region of the boundary. Therefore, the error estimator is applicable to a variety of physical problems. The error estimator is incorporated into an hp -adaptive finite element solver and verified against smooth and non-smooth problems with closed-form analytical solutions, as well as, being demonstrated on a non-smooth problem with complex boundary conditions. The hp -adaptive finite element analyses achieve exponential rates of convergence. The performances of the hp -adaptive scheme are contrasted against uniform and adaptive h refinement. This paper provides a complete framework for adaptivity in the symmetric interior penalty discontinuous Galerkin finite element method for linear elastic analysis.

© 2018 The Author(s). Published by Elsevier Inc.
This is an open access article under the CC BY license.
(<http://creativecommons.org/licenses/by/4.0/>)

1. Introduction

The discretization of partial differential equations for numerical computation facilitates the solution of physical systems, however, it introduces approximation errors. Error estimators are essential for the numerical analysis of boundary value problems as they allow for the assessment of the accuracy of a simulation in the absence of analytical solutions [1].

In this work, we present a new error estimator for linear elasticity based on a Discontinuous Galerkin (DG) finite element method. DG methods were introduced in the early 1970s as a way to numerically solve first-order hyperbolic problems [2]. More recently, these methods have been applied to elliptic problems [3–5]. A variety of DG methods have been developed in the decades [6], among them is the subclass of interior penalty DG methods which are stable and, in the authors' opinion, easy to implement. For these reasons the method used in this work is the symmetric version of the interior penalty DG method.

Error estimators for elliptic problems have been an important topic in the last few years. In [7] the first residual-based energy-norm error estimator for the symmetric interior penalty discontinuous Galerkin finite element method is presented. In the following years, inspired by this pioneering work, error estimators have been derived to solve a variety of problems

* Corresponding author.

E-mail addresses: robert.e.bird@durham.ac.uk (R.E. Bird), w.m.coombs@durham.ac.uk (W.M. Coombs), stefano.giani@durham.ac.uk (S. Giani).

(see for example [8–11]). The present work is meant to fill the need of an *hp* residual-based energy-norm error estimator for DG methods for linear elasticity.

The layout of the paper is as follows. Section 2 introduces the linear elastic model problem including pure Neumann/Dirichlet and mixed Neumann/Dirichlet boundary conditions and Section 3 presents the weak formulation for this problem. The symmetric interior penalty discontinuous Galerkin finite element method is introduced in Section 4, and Section 5 provides the a priori convergence results of the method. Sections 6 and 7 present the reliability and the efficiency of the error estimator. The analysis in Sections 6 and 7 is only presented for the two dimensional case, but it holds also for the three dimensional case. The restriction to the two dimensional case is to keep the paper more readable. For the same reason we only consider triangular elements, but the analysis is also applicable to affine quadrilateral elements and to tetrahedral and affine hexahedral elements in three dimensions. Numerical examples verifying the error estimator and its implementation within an *hp*-adaptive solver are presented in Section 8 before conclusions are drawn in Section 9.

2. Model problem

The model problem considered in this paper is linear elasticity with several kinds of boundary conditions: let Ω be a bounded polygonal domain in \mathbb{R}^2 with $\partial\Omega = \Gamma_D \cup \Gamma_N \cup \Gamma_T$, where Γ_D , Γ_N and Γ_T are disjoint sets, and let \mathbf{u} the solution of

$$\begin{aligned} -\nabla \cdot \boldsymbol{\sigma}(\mathbf{u}) &= \mathbf{f} \text{ in } \Omega, \\ \mathbf{u} &= \mathbf{g}_D \text{ on } \Gamma_D, \\ \boldsymbol{\sigma}(\mathbf{u}) \cdot \mathbf{n} &= \mathbf{g}_N \text{ on } \Gamma_N, \\ \mathbf{u} \cdot \mathbf{n} &= \mathbf{g}_T \cdot \mathbf{n} \text{ on } \Gamma_T, \\ \mathbf{t}(\mathbf{u}) \cdot \mathbf{n}_{\parallel} &= 0 \text{ on } \Gamma_T, \end{aligned} \tag{1}$$

with $\mathbf{u} \in [H^1(\Omega)]^2$ and where $\mathbf{n} = (n_x, n_y)$ is the unit vector perpendicular to the boundary of Ω and pointing out and \mathbf{n}_{\parallel} is the tangential unit vectors to the boundary, $\mathbf{t}(\mathbf{u})$ is the traction component of the stress, i.e.

$$\mathbf{t}(\mathbf{u}) := \boldsymbol{\sigma}(\mathbf{u}) \cdot \mathbf{n}$$

and where \mathbf{f} , \mathbf{g}_D , \mathbf{g}_N and \mathbf{g}_T are functions respectively in $[L^2(\Omega)]^2$, $[H^{1/2}(\Gamma_D)]^2$, $[L^2(\Gamma_N)]^2$ and $[H^{1/2}(\Gamma_T)]^2$. The last equation in (1) imposes that the tangential component of the traction is zero.

In order to ensure that the model problem (1) has a unique solution, the rigid motions have to be excluded. In order to do that lets introduce the function space $\mathcal{S} := [H^1(\Omega)]^2 \setminus R$, where R is the space containing all rigid motions, clearly rigid motions are not in \mathcal{S} . In view of this we assume that $\mathbf{u} \in \mathcal{S}$. The lack of uniqueness of the solution can be traced to the fact that the kernel of the strain operator $\boldsymbol{\epsilon}(\cdot)$ contains only rigid motions [12].

Remark 1. One or more sets among Γ_D , Γ_N and Γ_T can be empty. We assume that all the considered combinations of boundary conditions ensure the uniqueness of the solution of problem (1) up to rigid motions. A way to filter out the rigid motions in simulations is presented in [13]. This technique is used in Section 8.3 to solve the crack in a plate problem.

We define the strain tensor for a displacement \mathbf{v} as $\boldsymbol{\epsilon}(\mathbf{v})_{ij} := \frac{1}{2}(\nabla_j v_i + \nabla_i v_j)$ and we restrict the choice of material properties such that we have that $\boldsymbol{\sigma}(\mathbf{v}) = \mathbf{D}\boldsymbol{\epsilon}(\mathbf{v})$ where the matrix $\mathbf{D} \in \mathbb{R}^{3 \times 3 \times 3 \times 3}$ is symmetric and invertible implying that there are two positive constants D_{\min} and D_{\max} such that

$$D_{\min} |\mathbf{x}| \leq |\mathbf{D}\mathbf{x}| \leq D_{\max} |\mathbf{x}|, \quad \forall \mathbf{x} \in \mathbb{R}^{3 \times 3}. \tag{2}$$

It is straightforward to see that on \mathcal{S} there are two positive constants c_{ϵ} and C_{ϵ} such that

$$c_{\epsilon} \|\nabla \mathbf{v}\|_{0,\Omega} \leq \|\boldsymbol{\epsilon}(\mathbf{v})\|_{0,\Omega} \leq C_{\epsilon} \|\nabla \mathbf{v}\|_{0,\Omega}, \quad \forall \mathbf{v} \in \mathcal{S}, \tag{3}$$

with $\|\cdot\|_{0,\Omega}$ the L^2 norm. Also, thanks to the fact that D is invertible, there are two positive constants c_{σ} and C_{σ} such that

$$c_{\sigma} \|\nabla \mathbf{v}\|_{0,\Omega} \leq \|\boldsymbol{\sigma}(\mathbf{v})\|_{0,\Omega} \leq C_{\sigma} \|\nabla \mathbf{v}\|_{0,\Omega}, \quad \forall \mathbf{v} \in \mathcal{S}. \tag{4}$$

Theorem 2.1 (Coercivity in the continuous case). *There is a positive constant c_{CG} such that for any function $\mathbf{v} \in \mathcal{S}$ we have:*

$$\|\nabla \mathbf{v}\|_{0,\Omega}^2 \leq c_{CG} \left| \int_{\Omega} \boldsymbol{\sigma}(\mathbf{v}) : \boldsymbol{\epsilon}(\mathbf{v}) \, d\mathbf{x} \right|.$$

Proof. The statement comes easily from (3) and (4). \square

3. Continuous weak formulation

In this section we introduce the continuous weak formulation of problem (1), this formulation is only used in the analysis for the error estimator and it is not implemented in the code. Due to the variety of boundary conditions in (1), we introduce different spaces for the trial and test functions:

$$\mathcal{S}_1^{CG} := \{\mathbf{u} \in \mathcal{S} : \mathbf{u}|_{\Gamma_D} = \mathbf{g}_D, \mathbf{u} \cdot \mathbf{n}|_{\Gamma_T} = \mathbf{g}_T \cdot \mathbf{n}\}, \tag{5}$$

$$S_2^{CG} := \{\mathbf{v} \in S : \mathbf{v}|_{\Gamma_D} = \mathbf{0}, \quad \mathbf{v} \cdot \mathbf{n}|_{\Gamma_T} = 0\}, \tag{5}$$

with \mathbf{n} the unit vector perpendicular to the boundary of Ω and pointing outward.

Thus, the weak form of problem (1) reads as follows: find $\mathbf{u} \in S_1^{CG}$ such that

$$a^{CG}(\mathbf{u}, \mathbf{v}) = l^{CG}(\mathbf{v}) \quad \forall \mathbf{v} \in S_2^{CG}, \tag{6}$$

where the bilinear form $a^{CG}(\cdot, \cdot)$ and the linear form $l^{CG}(\cdot)$ are

$$\begin{aligned} a^{CG}(\mathbf{u}, \mathbf{v}) &:= \int_{\Omega} \boldsymbol{\sigma}(\mathbf{u}) : \boldsymbol{\epsilon}(\mathbf{v}) \, d\mathbf{x}, \\ l^{CG}(\mathbf{v}) &:= \int_{\Omega} \mathbf{f} \cdot \mathbf{v} \, d\mathbf{x} + \int_{\Gamma_N} \mathbf{g}_N \cdot \mathbf{v} \, ds. \end{aligned} \tag{7}$$

The definitions in (7) can be derived from the strong problem (1) applying integration by parts and then applying the boundary conditions.

4. Symmetric interior penalty discontinuous Galerkin method

In this section, we introduce our DG method to solve problem (1) on Ω . Throughout, we assume that the computational domain Ω can be partitioned into a shape regular mesh \mathcal{T} of triangular elements and we denote with K a generic element of \mathcal{T} . Also we assume that the elements are affine, i.e. for each element K there exists an affine map between the reference element \hat{K} and the physical element K . We allow for a maximum of one hanging node per edge and we denote $\mathcal{E}(\mathcal{T})$ and $\mathcal{E}^{int}(\mathcal{T}) \subset \mathcal{E}(\mathcal{T})$ the set of all edges of the mesh \mathcal{T} and the subset of all interior edges, respectively, and by $\mathcal{E}^{BC}(\mathcal{T}) \subset \mathcal{E}(\mathcal{T})$ the subset of all boundary edges. Furthermore, the set $\mathcal{E}^{BC}(\mathcal{T})$ is partitioned in the three subsets $\mathcal{E}^D(\mathcal{T})$, $\mathcal{E}^N(\mathcal{T})$ and $\mathcal{E}^T(\mathcal{T})$ that are the sets containing the edges forming the three portions of the boundary Γ_D , Γ_N and Γ_T . We define h_K and h_E to be the diameter of the element K and the length of the edge E respectively and we also define h_{max} as the maximum of h_K on the mesh \mathcal{T} .

Now we introduce the polynomial degrees for the approximation in our DG method. Hence, for each element K of the mesh \mathcal{T} we associate a polynomial degree $p_K \geq 1$ and we introduce the degree vector $\mathbf{p} = \{p_K : K \in \mathcal{T}\}$ and we define p_{min} as the minimum of p_K on the mesh \mathcal{T} . We assume that \mathbf{p} is of bounded local variation on all meshes in the sense that for any pair of neighbouring elements $K, K' \in \mathcal{T}$, we have

$$\varrho^{-1} \leq \frac{p_K}{p_{K'}} \leq \varrho, \tag{8}$$

where $\varrho \geq 1$ is a constant independent of the particular mesh. For any $E \in \mathcal{E}(\mathcal{T})$, we introduce the edge polynomial degree p_E by

$$p_E = \begin{cases} \max(p_K, p_{K'}), & \text{if } E = \partial K \cap \partial K', \ E \in \mathcal{E}^{int}(\mathcal{T}), \\ p_K, & \text{if } E = \partial K \cap \partial \Omega, \ E \in \mathcal{E}(\mathcal{T}) \setminus \mathcal{E}^{int}(\mathcal{T}). \end{cases} \tag{9}$$

Hence, for a given partition \mathcal{T} of Ω and a degree vector \mathbf{p} on \mathcal{T} , we define the hp -version DG finite element space by

$$V_{\mathbf{p}}(\mathcal{T}) = \left\{ \mathbf{v} \in [L^2(\Omega)]^2 \setminus R : \mathbf{v}|_K \in [\mathcal{P}_{p_K}(K)]^2, \quad K \in \mathcal{T} \right\}, \tag{10}$$

where $\mathcal{P}_{p_K}(K)$ is the space of polynomials of degree at most p_K and R is the set of rigid motions, see Remark 1. The exclusion of rigid motions from the DG space is useful for the analysis. In practice this constraint is imposed as explained in Remark 1.

Given an edge $E \in \mathcal{E}^{int}(\mathcal{T})$ shared by two elements K^+ and K^- , we define denoting with $+$ and $-$ the values from the two elements. Moreover, we define $\mathbf{n}_K^+ = (n_x^+, n_y^+)$ the outward unit normal on the boundary ∂K^+ of an element K , then we define the jump $[[\cdot]]$ operator and the average $\{ \cdot \}$ operator on vectors and tensors as:

$$\begin{aligned} [[\mathbf{v}]]_{ij} &= \mathbf{v}_i^+ \mathbf{n}_{Kj}^+ - \mathbf{v}_i^- \mathbf{n}_{Kj}^+, \\ [[\boldsymbol{\sigma}]]_i &= \boldsymbol{\sigma}_{ij}^+ \mathbf{n}_{Kj}^+ - \boldsymbol{\sigma}_{ij}^- \mathbf{n}_{Kj}^+, \\ \{\boldsymbol{\sigma}(\mathbf{v})\} &= \frac{1}{2}(\boldsymbol{\sigma}(\mathbf{v})^+ + \boldsymbol{\sigma}(\mathbf{v})^-). \end{aligned} \tag{11}$$

Note that if $E \subset \partial \Omega$, we set $\{\boldsymbol{\sigma}(\mathbf{v})\} = \boldsymbol{\sigma}(\mathbf{v})$, $[[\boldsymbol{\sigma}]]_i = \boldsymbol{\sigma}_{ij} \mathbf{n}_{Kj}^+$ and $[[\mathbf{v}]]_{ij} = \mathbf{v}_i \mathbf{n}_{Kj}^+$. Thus, the DG approximation problem (1) reads as follows: find $\mathbf{u}_h \in V_{\mathbf{p}}(\mathcal{T})$ such that

$$a^{DG}(\mathbf{u}_h, \mathbf{v}_h) = l(\mathbf{v}_h), \quad \forall \mathbf{v}_h \in V_{\mathbf{p}}(\mathcal{T}), \tag{12}$$

where the bilinear form

$$\begin{aligned}
 a^{\text{DG}}(\mathbf{u}, \mathbf{v}) &:= \sum_{K \in \mathcal{T}} \int_K \boldsymbol{\sigma}(\mathbf{u}) : \boldsymbol{\epsilon}(\mathbf{v}) \, dx \\
 &\quad - \sum_{E \in \mathcal{E}^{\text{int}}(\mathcal{T}) \cup \mathcal{E}^{\text{D}}(\mathcal{T})} \int_E \{ \boldsymbol{\sigma}(\mathbf{u}) \} : [\mathbf{v}] + \{ \boldsymbol{\sigma}(\mathbf{v}) \} : [\mathbf{u}] \, ds \\
 &\quad + \sum_{E \in \mathcal{E}^{\text{int}}(\mathcal{T}) \cup \mathcal{E}^{\text{D}}(\mathcal{T})} \frac{\gamma p_E^2}{h_E} \int_E [[\mathbf{u}]] : [[\mathbf{v}]] \, ds \\
 &\quad - \sum_{E \in \mathcal{E}^{\text{T}}(\mathcal{T})} \int_E (\mathbf{t}(\mathbf{u}) \cdot \mathbf{n})(\mathbf{v} \cdot \mathbf{n}) + (\mathbf{t}(\mathbf{v}) \cdot \mathbf{n})(\mathbf{u} \cdot \mathbf{n}) \, ds \\
 &\quad + \sum_{E \in \mathcal{E}^{\text{T}}(\mathcal{T})} \frac{\gamma p_E^2}{h_E} \int_E (\mathbf{u} \cdot \mathbf{n})(\mathbf{v} \cdot \mathbf{n}) \, ds,
 \end{aligned}$$

and the linear form

$$\begin{aligned}
 l(\mathbf{v}) &:= \sum_{K \in \mathcal{T}} \int_K \mathbf{f} \cdot \mathbf{v} \, dx - \sum_{E \in \mathcal{E}^{\text{D}}(\mathcal{T})} \int_E \mathbf{g}_D \cdot \boldsymbol{\sigma}(\mathbf{v}) \cdot \mathbf{n} \, ds + \sum_{E \in \mathcal{E}^{\text{D}}(\mathcal{T})} \frac{\gamma p_E^2}{h_E} \int_E \mathbf{g}_D \cdot \mathbf{v} \, ds + \sum_{E \in \mathcal{E}^{\text{N}}(\mathcal{T})} \int_E \mathbf{g}_N \cdot \mathbf{v} \, ds \\
 &\quad - \sum_{E \in \mathcal{E}^{\text{T}}(\mathcal{T})} \int_E (\mathbf{g}_T \cdot \mathbf{n})(\mathbf{t}(\mathbf{v}) \cdot \mathbf{n}) \, ds + \sum_{E \in \mathcal{E}^{\text{T}}(\mathcal{T})} \frac{\gamma p_E^2}{h_E} \int_E (\mathbf{g}_T \cdot \mathbf{n})(\mathbf{v} \cdot \mathbf{n}) \, ds
 \end{aligned}$$

where γ is the penalty constant.

The natural norm for problem (12) is the DG norm:

$$\| | \mathbf{u} | \|_{\mathcal{T}} := \left(\sum_{K \in \mathcal{T}} \| \nabla \mathbf{u} \|_{0,K}^2 + \sum_{E \in \mathcal{E}^{\text{int}}(\mathcal{T})} \frac{\gamma p_E^2}{h_E} \| [[\mathbf{u}]] \|_{0,E}^2 + \sum_{E \in \mathcal{E}^{\text{D}}(\mathcal{T})} \frac{\gamma p_E^2}{h_E} \| \mathbf{u} \|_{0,E}^2 + \sum_{E \in \mathcal{E}^{\text{T}}(\mathcal{T})} \frac{\gamma p_E^2}{h_E} \| \mathbf{u} \cdot \mathbf{n} \|_{0,E}^2 \right)^{1/2}, \tag{13}$$

where $\| \cdot \|_{0,K}$ and $\| \cdot \|_{0,E}$ are respectively the L^2 -norm on an element K and on an edge E .

5. A priori convergence results

In this section, we prove the a priori convergence of the DG method. For this purpose we need to introduce an additional function space:

$$[H^s(\mathcal{T})]^2 := \{ \mathbf{v} \in [L^2(\Omega)]^2 : \mathbf{v}|_K \in [H^s(K)]^2, K \in \mathcal{T} \}.$$

Remark 2. From now on the notation $a \lesssim b$ is used to denote $a \leq cb$, where c is a constant that may depend on the coefficients in (1), the value of γ and the constant in Theorem 2.1. The constant c is always independent of the sizes of the elements and the orders of polynomials in the elements.

Lemma 1. Let $K \in \mathcal{T}$ be a triangular element and \mathbf{u} a function in $[H^s(K)]^2$, with $s \geq 1$. There exists a positive constant C_π depending on s and on the shape regularity of the mesh but independent of \mathbf{u} , p_K and h_K , and a polynomial $\pi \mathbf{u} \in [\mathcal{P}_{p_K}(K)]^2$, with $p_K \geq 1$, such that for any q , $0 \leq q \leq s$

$$\| \mathbf{u} - \pi \mathbf{u} \|_{q,K} \leq C_\pi \frac{h_K^{\mu-q}}{p_K^{s-q}} \| \mathbf{u} \|_{s,K}, \tag{14}$$

$$\| \mathbf{u} - \pi \mathbf{u} \|_{0,E} \leq C_\pi \frac{h_K^{\mu-1/2}}{p_K^{s-1/2}} \| \mathbf{u} \|_{s,K}, \tag{15}$$

where $\mu = \min(p_K + 1, s)$ and where $E \subset \partial K$.

This result for the scalar case is presented in Lemma A.7 in [14]. The definition of the projection operator is in [15] for the p -case and in [16] for the hp -case. The extension of the operator from the scalar case to the vector case is trivial and it consists in applying the operator to each component of the vector function \mathbf{u} .

Theorem 5.1. Let $\mathbf{u} \in S \cap [H^s(\mathcal{T})]^2$, with $s \geq 2$, be a solution of (1) and \mathbf{u}_h the corresponding DG approximation. Then choosing γ large enough we have:

$$\| | \mathbf{u} - \mathbf{u}_h | \|_{\mathcal{T}} \lesssim \frac{h_{\max}^{\mu-1}}{p_{\min}^{s-3/2}} \| \mathbf{u} \|_{s,\Omega},$$

where h_{\max} and p_{\min} are defined in Section 4 and where $\mu = \min(p_{\min} + 1, s)$ and $p_{\min} \geq 1$.

Proof. The proof is based on [14, Theorem 4.1], but in order to apply it to linear elasticity, we extended it in several ways including to remove rigid motions. First we need to introduce a second DG norm:

$$\|\mathbf{u}\|_{\text{DG},\mathcal{T}}^2 := \|\mathbf{u}\|_{\mathcal{T}}^2 + \sum_{E \in \mathcal{E}^{\text{int}}(\mathcal{T}) \cup \mathcal{E}^{\text{D}}(\mathcal{T})} \int_E \frac{h_E}{\gamma p_E^2} |\{\boldsymbol{\sigma}(\mathbf{u}) \cdot \mathbf{n}\}|^2 ds + \sum_{E \in \mathcal{E}^{\Gamma}(\mathcal{T})} \int_E \frac{h_E}{\gamma p_E^2} |\{\mathbf{t}(\mathbf{u}) \cdot \mathbf{n}\}|^2 ds,$$

it is straightforward to see that $\|\cdot\|_{\text{DG},\mathcal{T}} \leq \|\cdot\|_{\text{DG},\mathcal{T}}$. Also Theorem 3.3 in [14] can be used to prove the continuity result in our case, i.e.

$$|a^{\text{DG}}(\mathbf{u}, \mathbf{v})| \lesssim \|\mathbf{u}\|_{\text{DG},\mathcal{T}} \|\mathbf{v}\|_{\text{DG},\mathcal{T}}, \quad \forall \mathbf{u}, \mathbf{v} \in [H^2(\mathcal{T})]^2 \setminus R. \tag{16}$$

Moreover, Theorem 3.5 in [14] can be used to prove the coercivity result in our case, i.e.

$$\|\mathbf{v}_h\|_{\text{DG},\mathcal{T}}^2 \lesssim a^{\text{DG}}(\mathbf{v}_h, \mathbf{v}_h), \quad \forall \mathbf{v}_h \in V_{\mathbf{p}}(\mathcal{T}). \tag{17}$$

Using the interpolation operator defined in Lemma 1, we have:

$$\|\mathbf{u} - \mathbf{u}_h\|_{\text{DG},\mathcal{T}} \leq \|\mathbf{u} - \pi\mathbf{u}\|_{\text{DG},\mathcal{T}} + \|\pi\mathbf{u} - \mathbf{u}_h\|_{\text{DG},\mathcal{T}},$$

then by (17) and the orthogonality of the DG solution, i.e. $a^{\text{DG}}(\mathbf{u} - \mathbf{u}_h, \mathbf{v}_h) = 0$, for all $\mathbf{v}_h \in V_{\mathbf{p}}(\mathcal{T})$, we have

$$\|\pi\mathbf{u} - \mathbf{u}_h\|_{\text{DG},\mathcal{T}}^2 \lesssim a^{\text{DG}}(\pi\mathbf{u} - \mathbf{u}_h, \pi\mathbf{u} - \mathbf{u}_h) = a^{\text{DG}}(\pi\mathbf{u} - \mathbf{u}, \pi\mathbf{u} - \mathbf{u}_h).$$

Furthermore applying (16) we obtain

$$\|\pi\mathbf{u} - \mathbf{u}_h\|_{\text{DG},\mathcal{T}} \lesssim \|\mathbf{u} - \pi\mathbf{u}\|_{\text{DG},\mathcal{T}}. \tag{18}$$

The result comes directly from (18) noticing that

$$\|\|\mathbf{u} - \mathbf{u}_h\|\|_{\mathcal{T}} \leq \|\mathbf{u} - \mathbf{u}_h\|_{\text{DG},\mathcal{T}} \lesssim \|\mathbf{u} - \pi\mathbf{u}\|_{\text{DG},\mathcal{T}}. \quad \square$$

The regularity assumption in Theorem 5.1 may be weakened using the same argument for the pure diffusion case as in [17].

6. Reliability of the error estimator

This section contains one of the main results of this paper which is the proof of reliability for the proposed error estimator (19). Theorem 6.1 guarantees that, up to a constant independent of the sizes of the elements or their order, the error estimator is an upper bound for the true error using the DG norm. This result is very useful in practice since the error estimator is computable also when the exact solution of a problem is not known, therefore it can be used to determine how accurate is the computed solution. Also, since the error estimator is computable, it can be used to drive adaptivity to improve the accuracy of the computed solution. In Section 8 a series of examples are presented to show the usage of the error estimator.

The error estimator presented in this paper is given by

$$\eta_{\text{err}} = \sqrt{\sum_{K \in \mathcal{T}} (\eta_{R,K}^2 + \eta_{J,K}^2 + \eta_{F,K}^2)}, \tag{19}$$

where the three terms under the sum are defined as

$$\begin{aligned} \eta_{R,K}^2 &:= \frac{h_K^2}{p_K^2} \left\| \mathbf{f}_h + \nabla \cdot \boldsymbol{\sigma}(\mathbf{u}_h) \right\|_{0,K}^2, \\ \eta_{J,K}^2 &:= \frac{1}{2} \sum_{E \in \mathcal{E}^{\text{int}}(K)} \frac{\gamma^2 p_E^3}{h_E} \left\| \llbracket \mathbf{u}_h \rrbracket \right\|_{0,E}^2 + \sum_{E \in \mathcal{E}^{\text{D}}(K)} \frac{\gamma^2 p_E^3}{h_E} \left\| \mathbf{u}_h - \mathbf{g}_{D,h} \right\|_{0,E}^2 + \sum_{E \in \mathcal{E}^{\Gamma}(K)} \frac{\gamma^2 p_E^3}{h_E} \left\| \mathbf{u}_h \cdot \mathbf{n} - \mathbf{g}_{T,h} \cdot \mathbf{n} \right\|_{0,E}^2, \\ \eta_{F,K}^2 &:= \frac{1}{2} \sum_{E \in \mathcal{E}^{\text{int}}(K)} \frac{h_E}{p_E} \left\| \llbracket \boldsymbol{\sigma}(\mathbf{u}_h) \rrbracket \right\|_{0,E}^2 + \sum_{E \in \mathcal{E}^{\text{N}}(K)} \frac{h_E}{p_E} \left\| \boldsymbol{\sigma}(\mathbf{u}_h) \cdot \mathbf{n} - \mathbf{g}_{N,h} \right\|_{0,E}^2 + \sum_{E \in \mathcal{E}^{\Gamma}(K)} \frac{h_E}{p_E} \left\| \mathbf{t}(\mathbf{u}_h) \cdot \mathbf{n} \right\|_{0,E}^2, \end{aligned}$$

where \mathbf{f}_h and $\mathbf{g}_{N,h}$ are the L^2 projections of \mathbf{f} and \mathbf{g}_N onto the finite element space and where $\mathbf{g}_{D,h}$ and $\mathbf{g}_{T,h}$ are approximated as in [18] of traces of functions in $H^1(\Omega)$ such that

$$\mathbf{g}_{D,h}|_E \in [\mathcal{P}_{p_K}(E)]^2, E \in \partial K \cap \Gamma_D, K \in \mathcal{T},$$

$$\mathbf{g}_{T,h}|_E \in [\mathcal{P}_{p_K}(E)]^2, E \in \partial K \cap \Gamma_T, K \in \mathcal{T},$$

and such that $\mathbf{g}_{D,h}$, $\mathbf{g}_{T,h}$ are on each edge E on the corresponding portions of the boundary the best approximations of \mathbf{g}_D , \mathbf{g}_T in the interpolation space $[(L^2(E), H^1(E))_{1/2}]^2$; we refer the reader to [19] and the references cited therein for details on the construction of the approximations and to [20] for the definition of the interpolation Sobolev space.

Due to the fact that data like \mathbf{f} or the values of the boundary conditions may not be represented exactly in the finite element space, the analysis include an oscillation term. This term is high order compared to η_{err} and for this reason is rarely computed in practice. Also the oscillation term is the sum of different terms:

$$\text{osc} := \sqrt{\text{osc}_{\text{glo}}^2 + \sum_{K \in \mathcal{T}} (\text{osc}_{R,K}^2 + \text{osc}_{J,K}^2 + \text{osc}_{F,K}^2)}, \quad (20)$$

where

$$\begin{aligned} \text{osc}_{\text{glo}}^2 &:= \|\mathbf{g}_D - \mathbf{g}_{D,h}\|_{1/2, \Gamma_D} + \|\mathbf{g}_N - \mathbf{g}_{N,h}\|_{0, \Gamma_N} + \|\mathbf{g}_T - \mathbf{g}_{T,h}\|_{1/2, \Gamma_T}, \\ \text{osc}_{R,K}^2 &:= \frac{h_K^2}{p_K^2} \|\mathbf{f} - \mathbf{f}_h\|_{0,K}^2, \\ \text{osc}_{J,K}^2 &:= \sum_{E \in \mathcal{E}^D(K)} \frac{\gamma^2 p_E^3}{h_E} \|\mathbf{g}_D - \mathbf{g}_{D,h}\|_{0,E}^2 + \sum_{E \in \mathcal{E}^T(K)} \frac{\gamma^2 p_E^3}{h_E} \|\mathbf{g}_T \cdot \mathbf{n} - \mathbf{g}_{T,h} \cdot \mathbf{n}\|_{0,E}^2, \\ \text{osc}_{F,K}^2 &:= \sum_{E \in \mathcal{E}^N(K)} \frac{h_E}{p_E} \|\mathbf{g}_N - \mathbf{g}_{N,h}\|_{0,E}^2. \end{aligned}$$

Next, we introduce the reliability result, which is the main result of this section. In the repository [21] we included a document containing a longer and more detailed version of the proof that is too long to include here.

Theorem 6.1. *Let \mathbf{u} the exact solution and \mathbf{u}_h the computed solution, we have that*

$$\|\mathbf{u} - \mathbf{u}_h\|_{\mathcal{T}} \leq C(\eta_{\text{err}} + \text{osc}),$$

where C is a positive constant independent of the mesh nor the order of the elements used.

The rest of the section is devoted to the proof of Theorem 6.1. The proof is based on [18] where a reliability proof for an error estimator for the Laplace equation is presented. However, to prove Theorem 6.1 for linear elasticity, the approach has been changed to deal with the fact that the model problem is a system of equations. Also, the presence of many different boundary conditions increases considerably the number of terms to consider in the proof.

In order to carry out the analysis we need to introduce an auxiliary continuous problem similar to (1) which is only used in the analysis and never in computations:

$$\begin{aligned} -\nabla \cdot \boldsymbol{\sigma}(\tilde{\mathbf{u}}) &= \mathbf{f} \quad \text{in } \Omega \\ \tilde{\mathbf{u}} &= \mathbf{g}_{D,h} \quad \text{on } \Gamma_D \\ \boldsymbol{\sigma}(\tilde{\mathbf{u}}) \cdot \mathbf{n} &= \mathbf{g}_{N,h} \quad \text{on } \Gamma_N \\ \tilde{\mathbf{u}} \cdot \mathbf{n} &= \mathbf{g}_{T,h} \cdot \mathbf{n} \quad \text{on } \Gamma_T \\ \mathbf{t}(\tilde{\mathbf{u}}) \cdot \mathbf{n}_{\parallel} &= \mathbf{0} \quad \text{on } \Gamma_T, \end{aligned} \quad (21)$$

with $\tilde{\mathbf{u}} \in [H^1(\Omega)]^2$. Since linear elasticity is a linear problem and its solutions depended continuously on their data, we have

$$\|\nabla(\mathbf{u} - \tilde{\mathbf{u}})\|_{0,\Omega} \lesssim \|\mathbf{g}_D - \mathbf{g}_{D,h}\|_{1/2, \Gamma_D} + \|\mathbf{g}_N - \mathbf{g}_{N,h}\|_{0, \Gamma_N} + \|\mathbf{g}_T - \mathbf{g}_{T,h}\|_{1/2, \Gamma_T}. \quad (22)$$

The introduction of this auxiliary problem is essential in the analysis to isolate the oscillation term.

For DG methods, the construction of the upper bound for the DG norm using the error is done in two steps bounding separately the conforming and the non conforming part of the error. To this end, we define the space $V_{\mathbf{p}}^c(\mathcal{T}) \equiv V_{\mathbf{p}}(\mathcal{T}) \cap [H^1(\Omega)]^2$ which is a conforming version of the DG space. Then, we decompose the discontinuous Galerkin finite element space $V_{\mathbf{p}}(\mathcal{T}) = V_{\mathbf{p}}^c(\mathcal{T}) \oplus V_{\mathbf{p}}^{\perp}(\mathcal{T})$, where $V_{\mathbf{p}}^{\perp}(\mathcal{T})$ is the orthogonal complement of $V_{\mathbf{p}}^c(\mathcal{T})$ with respect to the DG norm (13). We also define $V_{\mathbf{p},0}^c(\mathcal{T})$ which is the subspace of $V_{\mathbf{p}}^c(\mathcal{T})$ containing functions satisfying the following boundary conditions imposed strongly: $\mathbf{u} = \mathbf{0}$ on Γ_D , $\boldsymbol{\sigma}(\mathbf{u}) \cdot \mathbf{n} = \mathbf{0}$ on Γ_N , $\mathbf{u} \cdot \mathbf{n} = 0$ on Γ_T and $\mathbf{t}(\mathbf{u}) \cdot \mathbf{n}_{\parallel} = \mathbf{0}$ on Γ_T . We also assume that there is an interpolation operator $I_{hp} : V_{\mathbf{p}}(\mathcal{T}) \rightarrow V_{\mathbf{p}}^c(\mathcal{T})$ that satisfy the following inequalities:

$$p_K^2 h_K^{-2} \|\mathbf{v} - I_{hp} \mathbf{v}\|_{0,K}^2 \lesssim \|\nabla \mathbf{v}\|_{0,K}^2, \quad (23)$$

$$\|\nabla(\mathbf{v} - I_{hp} \mathbf{v})\|_{0,K}^2 \lesssim \|\nabla \mathbf{v}\|_{0,K}^2, \quad (24)$$

$$p_E h_E^{-1} \|\mathbf{v} - I_{hp} \mathbf{v}\|_{0,E}^2 \lesssim \|\nabla \mathbf{v}\|_{0,K}^2, \quad (25)$$

with $E \subset \partial K$. Examples of similar interpolation operators are the Scott–Zhang presented in [22] and used in [18] or the operator in [8].

We can then split the solution as:

$$\mathbf{u}_h - I_{hp} \tilde{\mathbf{u}} = \mathbf{u}_h^c + \mathbf{u}_h^r, \quad (26)$$

with $\mathbf{u}_h^c \in V_{\mathbf{p},0}^c(\mathcal{T})$ and $\mathbf{u}_h^r \in V_{\mathbf{p}}^\perp(\mathcal{T})$, then using the triangle inequality and (26), we obtain

$$\begin{aligned} |||\mathbf{u} - \mathbf{u}_h|||_{\mathcal{T}} &\leq |||\mathbf{u} - \tilde{\mathbf{u}}|||_{\mathcal{T}} + |||\tilde{\mathbf{u}} - \mathbf{u}_h|||_{\mathcal{T}} \\ &\leq |||\mathbf{u} - \tilde{\mathbf{u}}|||_{\mathcal{T}} + |||\tilde{\mathbf{u}} - I_{hp}\tilde{\mathbf{u}} - \mathbf{u}_h^c - \mathbf{u}_h^r|||_{\mathcal{T}} \\ &\leq |||\mathbf{u} - \tilde{\mathbf{u}}|||_{\mathcal{T}} + |||\tilde{\mathbf{u}} - I_{hp}\tilde{\mathbf{u}} - \mathbf{u}_h^c|||_{\mathcal{T}} + |||\mathbf{u}_h^r|||_{\mathcal{T}}. \end{aligned} \tag{27}$$

The first term on the rhs of (27) can be bounded using (22) and (13) noticing that $\mathbf{u} - \tilde{\mathbf{u}}$ is zero on the internal edges:

$$|||\mathbf{u} - \tilde{\mathbf{u}}|||_{\mathcal{T}}^2 = \|\nabla(\mathbf{u} - \tilde{\mathbf{u}})\|_{0,\Omega}^2 + \sum_{E \in \mathcal{E}^D(\mathcal{T})} \frac{\gamma p_E^2}{h_E} \|\mathbf{g}_D - \mathbf{g}_{D,h}\|_{0,E}^2 + \sum_{E \in \mathcal{E}^T(\mathcal{T})} \frac{\gamma p_E^2}{h_E} \|(\mathbf{g}_T - \mathbf{g}_{T,h}) \cdot \mathbf{n}\|_{0,E}^2 \lesssim \text{osc}^2. \tag{28}$$

Then, in order to obtain the upper bound for the conforming part of the error $|||\tilde{\mathbf{u}} - I_{hp}\tilde{\mathbf{u}} - \mathbf{u}_h^c|||_{\mathcal{T}}$, we recognize that $[[\tilde{\mathbf{u}} - I_{hp}\tilde{\mathbf{u}} - \mathbf{u}_h^c]] = 0$ in the interior of the mesh and so denoting

$$D(\mathbf{u}, \mathbf{v}) := \sum_{K \in \mathcal{T}} \int_K \boldsymbol{\sigma}(\mathbf{u}) : \boldsymbol{\epsilon}(\mathbf{v}) \, dx + \sum_{E \in \mathcal{E}^{\text{int}}(\mathcal{T}) \cup \mathcal{E}^D(\mathcal{T})} \frac{\gamma p_E^2}{h_E} \int_E [[\mathbf{u}]] : [[\mathbf{v}]] \, ds + \sum_{E \in \mathcal{E}^T(\mathcal{T})} \frac{\gamma p_E^2}{h_E} \int_E (\mathbf{u} \cdot \mathbf{n})(\mathbf{v} \cdot \mathbf{n}) \, ds, \tag{29}$$

we obtain from Theorem 2.1:

$$|||\tilde{\mathbf{u}} - I_{hp}\tilde{\mathbf{u}} - \mathbf{u}_h^c|||_{\mathcal{T}}^2 \lesssim D(\tilde{\mathbf{u}} - I_{hp}\tilde{\mathbf{u}} - \mathbf{u}_h^c, \tilde{\mathbf{u}} - I_{hp}\tilde{\mathbf{u}} - \mathbf{u}_h^c). \tag{30}$$

Then setting

$$\mathbf{v} = \frac{\tilde{\mathbf{u}} - I_{hp}\tilde{\mathbf{u}} - \mathbf{u}_h^c}{|||\tilde{\mathbf{u}} - I_{hp}\tilde{\mathbf{u}} - \mathbf{u}_h^c|||_{\mathcal{T}}} \in V_{\mathbf{p},0}^c(\mathcal{T}), \tag{31}$$

we have

$$\begin{aligned} |||\tilde{\mathbf{u}} - I_{hp}\tilde{\mathbf{u}} - \mathbf{u}_h^c|||_{\mathcal{T}} &\lesssim D(\tilde{\mathbf{u}} - I_{hp}\tilde{\mathbf{u}} - \mathbf{u}_h^c, \mathbf{v}) = D(\tilde{\mathbf{u}} - \mathbf{u}_h, \mathbf{v}) + D(\mathbf{u}_h^r, \mathbf{v}) \\ &= D(\mathbf{u} - \mathbf{u}_h, \mathbf{v}) + D(\tilde{\mathbf{u}} - \mathbf{u}, \mathbf{v}) + D(\mathbf{u}_h^r, \mathbf{v}). \end{aligned} \tag{32}$$

The term $D(\tilde{\mathbf{u}} - \mathbf{u}, \mathbf{v})$ can be bounded using the Cauchy–Schwarz inequality and (28) by

$$D(\tilde{\mathbf{u}} - \mathbf{u}, \mathbf{v}) \lesssim |||\mathbf{u} - \tilde{\mathbf{u}}|||_{\mathcal{T}} |||\mathbf{v}|||_{\mathcal{T}} \lesssim \text{osc} |||\mathbf{v}|||_{\mathcal{T}}. \tag{33}$$

To bound the term $D(\mathbf{u}_h^r, \mathbf{v})$ we use the next lemma:

Lemma 2. *Considering \mathbf{u}_h the DG solution of problem (12), we have*

$$|||\mathbf{u}_h^r|||_{\mathcal{T}} \lesssim \eta_{\text{err}}.$$

recalling that $\mathbf{u}_h^r = \mathbf{u}_h - I_{hp}\tilde{\mathbf{u}} - \mathbf{u}_h^c$.

Proof. From the definition of the DG norm (13) and the fact that $[[\mathbf{u}_h^r]] = [[\mathbf{u}_h]]$ on the edges in the interior:

$$|||\mathbf{u}_h^r|||_{\mathcal{T}}^2 = \sum_{K \in \mathcal{T}} \|\nabla \mathbf{u}_h^r\|_{0,K}^2 + \sum_{E \in \mathcal{E}^{\text{int}}(\mathcal{T}) \cup \mathcal{E}^D(\mathcal{T})} \frac{\gamma p_E^2}{h_E} \|[[\mathbf{u}_h]]\|_{0,E}^2 + \sum_{E \in \mathcal{E}^T(\mathcal{T})} \frac{\gamma p_E^2}{h_E} \|\mathbf{u}_h \cdot \mathbf{n}\|_{0,E}^2. \tag{34}$$

The next step is to bound the H^1 -seminorm of \mathbf{u}_h^r using the jump over the faces. Similar results have been already used in other works, like in [18]. However, such results are for problems with only Dirichlet type boundary conditions, which means that they are not suitable in this context. We need to bound the H^1 -seminorm of \mathbf{u}_h^r using only the jump over interior faces and faces on the portion of the boundary where only Dirichlet type of boundary conditions are imposed. Such result is proved for scalar problems in Theorem 2.1(ii) in [23] and for the case $\Gamma_D \cup \Gamma_T = \emptyset$, which is admissible for our model problem, we use Theorem 2.1(iii) from [23]. Applying the results from [23] to our problem, we have that there exists a projection operator $\pi_{hp} : V_{\mathbf{p}}(\mathcal{T}) \rightarrow V_{\mathbf{p},0}^c(\mathcal{T})$ such that for any $\mathbf{v}_h \in V_{\mathbf{p}}(\mathcal{T})$ holds true

$$\sum_{K \in \mathcal{T}} \|\nabla(\mathbf{v}_h - \pi_{hp}\mathbf{v}_h)\|_{0,K}^2 \lesssim \sum_{E \in \mathcal{E}^{\text{int}}(\mathcal{T})} \int_E p_E^2 h_E^{-1} |[[\mathbf{v}_h]]|^2 \, ds + \sum_{E \in \mathcal{E}^D(\mathcal{T})} \int_E p_E^2 h_E^{-1} |\mathbf{v}_h|^2 \, ds + \sum_{E \in \mathcal{E}^T(\mathcal{T})} \int_E p_E^2 h_E^{-1} |\mathbf{v}_h \cdot \mathbf{n}|^2 \, ds, \tag{35}$$

where the faces on the boundary considered on the rhs are also the ones on Γ_T for just the normal component since for that component the boundary condition is of Dirichlet type.

Then, since any function $\mathbf{v}_h^r \in V_{\mathbf{p}}^\perp(\mathcal{T})$ can be seen as $\mathbf{v}_h^r = \mathbf{v}_h - \pi_{hp}\mathbf{v}_h$ for some $\mathbf{v}_h \in V_{\mathbf{p}}(\mathcal{T})$, we can apply (35) on the first term of (34) and have

$$\sum_{K \in \mathcal{T}} \|\nabla \mathbf{u}_h^r\|_{0,K}^2 \lesssim \sum_{E \in \mathcal{E}^{\text{int}}(\mathcal{T})} \int_E p_E^2 h_E^{-1} |[[\mathbf{u}_h]]|^2 \, ds + \sum_{E \in \mathcal{E}^D(\mathcal{T})} \int_E p_E^2 h_E^{-1} |\mathbf{u}_h|^2 \, ds + \sum_{E \in \mathcal{E}^T(\mathcal{T})} \int_E p_E^2 h_E^{-1} |\mathbf{u}_h \cdot \mathbf{n}|^2 \, ds \lesssim \sum_{K \in \mathcal{T}} \eta_{j,K}^2.$$

Also the other two terms can be bounded straightforwardly by $\sum_{K \in \mathcal{T}} \eta_{j,K}^2$. \square

Then the term $D(\mathbf{u}_h^r, \mathbf{v})$ can be bounded using the Cauchy–Schwarz inequality and Lemma 2 by

$$D(\mathbf{u}_h^r, \mathbf{v}) \lesssim |||\mathbf{u}_h^r|||_{\mathcal{T}} |||\mathbf{v}|||_{\mathcal{T}} \lesssim \eta_{\text{err}} |||\mathbf{v}|||_{\mathcal{T}}. \tag{36}$$

To bound the remaining term $D(\mathbf{u} - \mathbf{u}_h, \mathbf{v})$ we use the fact that problem (12) can be rewritten as

$$D(\mathbf{u}_h, \mathbf{v}_h) + K(\mathbf{u}_h, \mathbf{v}_h) = l(\mathbf{v}_h) = l^c(\mathbf{v}_h) + l^r(\mathbf{v}_h),$$

where $K(\mathbf{u}, \mathbf{v}) = a^{\text{DG}}(\mathbf{u}, \mathbf{v}) - D(\mathbf{u}, \mathbf{v})$ and where

$$\begin{aligned} l^c(\mathbf{v}) &:= \sum_{K \in \mathcal{T}} \int_K \mathbf{f} \cdot \mathbf{v} \, d\mathbf{x} + \sum_{E \in \mathcal{E}^{\text{N}}(\mathcal{T})} \int_E \mathbf{g}_N \cdot \mathbf{v} \, ds, \\ l^r(\mathbf{v}) &:= - \sum_{E \in \mathcal{E}^{\text{D}}(\mathcal{T})} \int_E \mathbf{g}_D \cdot \boldsymbol{\sigma}(\mathbf{v}) \cdot \mathbf{n} \, ds + \sum_{E \in \mathcal{E}^{\text{D}}(\mathcal{T})} \frac{\gamma p_E^2}{h_E} \int_E \mathbf{g}_D \cdot \mathbf{v} \, ds \\ &\quad - \sum_{E \in \mathcal{E}^{\text{T}}(\mathcal{T})} \int_E (\mathbf{g}_T \cdot \mathbf{n})(\mathbf{t}(\mathbf{v}) \cdot \mathbf{n}) \, ds + \sum_{E \in \mathcal{E}^{\text{T}}(\mathcal{T})} \frac{\gamma p_E^2}{h_E} \int_E (\mathbf{g}_T \cdot \mathbf{n})(\mathbf{v} \cdot \mathbf{n}) \, ds. \end{aligned}$$

Then, we have choosing \mathbf{v} as in (31) and using (1):

$$\begin{aligned} D(\mathbf{u} - \mathbf{u}_h, \mathbf{v}) &= l^c(\mathbf{v}) - D(\mathbf{u}_h, \mathbf{v}) \\ &= l^c(\mathbf{v} - \mathbf{v}_h) - l^r(\mathbf{v}_h) - D(\mathbf{u}_h, \mathbf{v} - \mathbf{v}_h) + K(\mathbf{u}_h, \mathbf{v}_h). \end{aligned} \tag{37}$$

The next lemma is fundamental to bound the conforming part of the error with the error estimator.

Lemma 3. *Considering \mathbf{u}_h the DG solution of problem (12) and for any continuous function \mathbf{v} with $\mathbf{v}_h := I_{\text{hp}} \mathbf{v}$, we have:*

$$l^c(\mathbf{v} - \mathbf{v}_h) - l^r(\mathbf{v}_h) - D(\mathbf{u}_h, \mathbf{v} - \mathbf{v}_h) + K(\mathbf{u}_h, \mathbf{v}_h) \lesssim (\eta_{\text{err}} + \text{osc}) |||\mathbf{v}|||_{\mathcal{T}}.$$

Proof. Applying integration by parts to the first term in $D(\mathbf{u}_h, \mathbf{v} - \mathbf{v}_h)$:

$$\begin{aligned} &l^c(\mathbf{v} - \mathbf{v}_h) - l^r(\mathbf{v}_h) - D(\mathbf{u}_h, \mathbf{v} - \mathbf{v}_h) + K(\mathbf{u}_h, \mathbf{v}_h) \\ &= l^c(\mathbf{v} - \mathbf{v}_h) - l^r(\mathbf{v}_h) - \sum_{K \in \mathcal{T}} \int_K \boldsymbol{\sigma}(\mathbf{u}_h) : \boldsymbol{\epsilon}(\mathbf{v} - \mathbf{v}_h) \, d\mathbf{x} \\ &\quad - \sum_{E \in \mathcal{E}^{\text{int}}(\mathcal{T}) \cup \mathcal{E}^{\text{D}}(\mathcal{T})} \frac{\gamma p_E^2}{h_E} \int_E [[\mathbf{u}_h]] : [[\mathbf{v} - \mathbf{v}_h]] \, ds \\ &\quad - \sum_{E \in \mathcal{E}^{\text{T}}(\mathcal{T})} \frac{\gamma p_E^2}{h_E} \int_E (\mathbf{u}_h \cdot \mathbf{n})(\mathbf{v} - \mathbf{v}_h) \cdot \mathbf{n} \, ds + K(\mathbf{u}_h, \mathbf{v}_h) \\ &= l^c(\mathbf{v} - \mathbf{v}_h) - l^r(\mathbf{v}_h) + \sum_{K \in \mathcal{T}} \int_K \nabla \cdot \boldsymbol{\sigma}(\mathbf{u}_h) \cdot (\mathbf{v} - \mathbf{v}_h) \, d\mathbf{x} \\ &\quad - \sum_{K \in \mathcal{T}} \int_{\partial K} \boldsymbol{\sigma}(\mathbf{u}_h) \cdot \mathbf{n}_K \cdot (\mathbf{v} - \mathbf{v}_h) \, ds \\ &\quad - \sum_{E \in \mathcal{E}^{\text{int}}(\mathcal{T}) \cup \mathcal{E}^{\text{D}}(\mathcal{T})} \frac{\gamma p_E^2}{h_E} \int_E [[\mathbf{u}_h]] : [[\mathbf{v} - \mathbf{v}_h]] \, ds \\ &\quad - \sum_{E \in \mathcal{E}^{\text{T}}(\mathcal{T})} \frac{\gamma p_E^2}{h_E} \int_E (\mathbf{u}_h \cdot \mathbf{n})(\mathbf{v} - \mathbf{v}_h) \cdot \mathbf{n} \, ds + K(\mathbf{u}_h, \mathbf{v}_h). \end{aligned} \tag{38}$$

The term $\sum_{K \in \mathcal{T}} \int_{\partial K} \boldsymbol{\sigma}(\mathbf{u}_h) \cdot \mathbf{n}_K \cdot (\mathbf{v} - \mathbf{v}_h) \, ds$ can be further treated in the standard way for DG:

$$\begin{aligned} \sum_{K \in \mathcal{T}} \int_{\partial K} \boldsymbol{\sigma}(\mathbf{u}_h) \cdot \mathbf{n}_K \cdot (\mathbf{v} - \mathbf{v}_h) \, ds &= \sum_{E \in \mathcal{E}^{\text{int}}(\mathcal{T})} \int_E \{\boldsymbol{\sigma}(\mathbf{u}_h)\} : [[\mathbf{v} - \mathbf{v}_h]] \, ds \\ &\quad + \sum_{E \in \mathcal{E}^{\text{BC}}(\mathcal{T})} \int_E \boldsymbol{\sigma}(\mathbf{u}_h) \cdot \mathbf{n}_K \cdot (\mathbf{v} - \mathbf{v}_h) \, ds + \sum_{E \in \mathcal{E}^{\text{int}}(\mathcal{T})} \int_E [[\boldsymbol{\sigma}(\mathbf{u}_h)]] \cdot \{\mathbf{v} - \mathbf{v}_h\} \, ds \\ &= - \sum_{E \in \mathcal{E}^{\text{int}}(\mathcal{T})} \int_E \{\boldsymbol{\sigma}(\mathbf{u}_h)\} : [[\mathbf{v}_h]] \, ds + \sum_{E \in \mathcal{E}^{\text{BC}}(\mathcal{T})} \int_E \boldsymbol{\sigma}(\mathbf{u}_h) \cdot \mathbf{n}_K \cdot (\mathbf{v} - \mathbf{v}_h) \, ds \\ &\quad + \sum_{E \in \mathcal{E}^{\text{int}}(\mathcal{T})} \int_E [[\boldsymbol{\sigma}(\mathbf{u}_h)]] \cdot \{\mathbf{v} - \mathbf{v}_h\} \, ds, \end{aligned}$$

where in the last step we used the fact that $[\mathbf{v}]] = \mathbf{0}$ in the interior of the mesh. Adding also the term $K(\mathbf{u}_h, \mathbf{v}_h)$ we have:

$$\begin{aligned} K(\mathbf{u}_h, \mathbf{v}_h) &- \sum_{K \in \mathcal{T}} \int_{\partial K} \boldsymbol{\sigma}(\mathbf{u}_h) \cdot \mathbf{n}_K \cdot (\mathbf{v} - \mathbf{v}_h) \, ds = - \sum_{E \in \mathcal{E}^{\text{int}}(\mathcal{T})} \int_E [[\mathbf{u}_h]] : \{\boldsymbol{\sigma}(\mathbf{v}_h)\} \, ds \\ &- \sum_{E \in \mathcal{E}^{\text{D}}(\mathcal{T})} \int_E \boldsymbol{\sigma}(\mathbf{u}_h) \cdot \mathbf{n}_K \cdot \mathbf{v}_h + \mathbf{u}_h \cdot \boldsymbol{\sigma}(\mathbf{v}_h) \cdot \mathbf{n}_K \, ds \\ &- \sum_{E \in \mathcal{E}^{\text{T}}(\mathcal{T})} \int_E (\mathbf{t}(\mathbf{u}_h) \cdot \mathbf{n})(\mathbf{v}_h \cdot \mathbf{n}) + (\mathbf{u}_h \cdot \mathbf{n})(\mathbf{t}(\mathbf{v}_h) \cdot \mathbf{n}) \, ds \\ &- \sum_{E \in \mathcal{E}^{\text{BC}}(\mathcal{T})} \int_E \boldsymbol{\sigma}(\mathbf{u}_h) \cdot \mathbf{n}_K \cdot (\mathbf{v} - \mathbf{v}_h) \, ds - \sum_{E \in \mathcal{E}^{\text{int}}(\mathcal{T})} \int_E [[\boldsymbol{\sigma}(\mathbf{u}_h)]] : \{\mathbf{v} - \mathbf{v}_h\} \, ds. \end{aligned}$$

In view of this, the rhs in Eq. (38) can be split in four terms defined as:

$$\begin{aligned} T_1 &:= \int_{\Omega} \mathbf{f} \cdot (\mathbf{v} - \mathbf{v}_h) + \nabla \cdot \boldsymbol{\sigma}(\mathbf{u}_h) \cdot (\mathbf{v} - \mathbf{v}_h) \, d\mathbf{x}, \\ T_2 &:= - \sum_{E \in \mathcal{E}^{\text{int}}(\mathcal{T}) \cup \mathcal{E}^{\text{D}}(\mathcal{T})} \frac{\gamma p_E^2}{h_E} \int_E [[\mathbf{u}_h]] : \{\mathbf{v} - \mathbf{v}_h\} \, ds - \sum_{E \in \mathcal{E}^{\text{T}}(\mathcal{T})} \frac{\gamma p_E^2}{h_E} \int_E (\mathbf{u}_h \cdot \mathbf{n})(\mathbf{v} - \mathbf{v}_h) \cdot \mathbf{n} \, ds \\ &- \sum_{E \in \mathcal{E}^{\text{D}}(\mathcal{T})} \frac{\gamma p_E^2}{h_E} \int_E \mathbf{g}_D \cdot \mathbf{v}_h \, ds - \sum_{E \in \mathcal{E}^{\text{T}}(\mathcal{T})} \frac{\gamma p_E^2}{h_E} \int_E (\mathbf{g}_T \cdot \mathbf{n})(\mathbf{v}_h \cdot \mathbf{n}) \, ds, \\ T_3 &:= - \sum_{E \in \mathcal{E}^{\text{int}}(\mathcal{T})} \int_E [[\boldsymbol{\sigma}(\mathbf{u}_h)]] : \{\mathbf{v} - \mathbf{v}_h\} \, ds \\ &- \sum_{E \in \mathcal{E}^{\text{D}}(\mathcal{T})} \int_E \boldsymbol{\sigma}(\mathbf{u}_h) \cdot \mathbf{n}_K \cdot (\mathbf{v} - \mathbf{v}_h) \, ds - \sum_{E \in \mathcal{E}^{\text{D}}(\mathcal{T})} \int_E \boldsymbol{\sigma}(\mathbf{u}_h) \cdot \mathbf{n}_K \cdot \mathbf{v}_h \, ds \\ &- \sum_{E \in \mathcal{E}^{\text{N}}(\mathcal{T})} \int_E \boldsymbol{\sigma}(\mathbf{u}_h) \cdot \mathbf{n}_K \cdot (\mathbf{v} - \mathbf{v}_h) \, ds + \sum_{E \in \mathcal{E}^{\text{N}}(\mathcal{T})} \int_E \mathbf{g}_N \cdot (\mathbf{v} - \mathbf{v}_h) \, ds \\ &- \sum_{E \in \mathcal{E}^{\text{T}}(\mathcal{T})} \int_E \boldsymbol{\sigma}(\mathbf{u}_h) \cdot \mathbf{n}_K \cdot (\mathbf{v} - \mathbf{v}_h) \, ds - \sum_{E \in \mathcal{E}^{\text{T}}(\mathcal{T})} \int_E (\mathbf{t}(\mathbf{u}_h) \cdot \mathbf{n})(\mathbf{v}_h \cdot \mathbf{n}) \, ds \\ T_4 &:= - \sum_{E \in \mathcal{E}^{\text{int}}(\mathcal{T})} \int_E [[\mathbf{u}_h]] \cdot \{\boldsymbol{\sigma}(\mathbf{v}_h)\} \, ds \\ &- \sum_{E \in \mathcal{E}^{\text{D}}(\mathcal{T})} \int_E \mathbf{u}_h \cdot \boldsymbol{\sigma}(\mathbf{v}_h) \cdot \mathbf{n}_K \, ds + \sum_{E \in \mathcal{E}^{\text{D}}(\mathcal{T})} \int_E \mathbf{g}_D \cdot \boldsymbol{\sigma}(\mathbf{v}_h) \cdot \mathbf{n}_K \, ds \\ &- \sum_{E \in \mathcal{E}^{\text{T}}(\mathcal{T})} \int_E (\mathbf{u}_h \cdot \mathbf{n})(\mathbf{t}(\mathbf{v}_h) \cdot \mathbf{n}) \, ds + \sum_{E \in \mathcal{E}^{\text{T}}(\mathcal{T})} \int_E (\mathbf{g}_T \cdot \mathbf{n})(\mathbf{t}(\mathbf{v}_h) \cdot \mathbf{n}) \, ds, \end{aligned}$$

The rest of the proof consists in bounding each term separately. To bound T_1 , we use the Cauchy–Schwarz inequality, (23) and $\mathbf{v}_h := I_{hp}\mathbf{v}$:

$$\begin{aligned} T_1 &\leq \left[\left(\sum_{K \in \mathcal{T}} \frac{h_K^2}{p_K^2} \|\mathbf{f}_h + \nabla \cdot \boldsymbol{\sigma}(\mathbf{u}_h)\|_{0,K}^2 \right)^{1/2} + \left(\sum_{K \in \mathcal{T}} \frac{h_K^2}{p_K^2} \|\mathbf{f} - \mathbf{f}_h\|_{0,K}^2 \right)^{1/2} \right] \\ &\quad \times \left(\sum_{K \in \mathcal{T}} \frac{p_K^2}{h_K^2} \|\mathbf{v} - \mathbf{v}_h\|_{0,K}^2 \right)^{1/2} \\ &\lesssim \left[\left(\sum_{K \in \mathcal{T}} \eta_{R,K}^2 \right)^{1/2} + \left(\sum_{K \in \mathcal{T}} \text{osc}_{R,K}^2 \right)^{1/2} \right] \|\mathbf{v}\|_{\mathcal{T}}. \end{aligned}$$

To bound T_2 , we use the Cauchy–Schwarz inequality, (25), the shape regularity assumption on the mesh \mathcal{T} and the facts that $\mathbf{v} = \mathbf{0}$ on Γ_D and $\mathbf{v} \cdot \mathbf{n} = \mathbf{0}$ on Γ_T :

$$\begin{aligned} T_2 &\leq \left[\left(\sum_{E \in \mathcal{E}^{\text{int}}(\mathcal{T})} \frac{\gamma^2 p_E^3}{h_E} \|[[\mathbf{u}_h]]\|_{0,E}^2 + \sum_{E \in \mathcal{E}^{\text{D}}(\mathcal{T})} \frac{\gamma^2 p_E^3}{h_E} \|\mathbf{u}_h - \mathbf{g}_{D,h}\|_{0,E}^2 \right. \right. \\ &\quad \left. \left. + \sum_{E \in \mathcal{E}^{\text{T}}(\mathcal{T})} \frac{\gamma^2 p_E^3}{h_E} \|\mathbf{u}_h \cdot \mathbf{n} - \mathbf{g}_{T,h} \cdot \mathbf{n}\|_{0,E}^2 \right)^{1/2} \right] \end{aligned}$$

$$\begin{aligned}
 & + \left(\sum_{E \in \mathcal{E}^D(\mathcal{T})} \frac{\gamma^2 p_E^3}{h_E} \|\mathbf{g}_D - \mathbf{g}_{D,h}\|_{0,E}^2 + \sum_{E \in \mathcal{E}^T(\mathcal{T})} \frac{\gamma^2 p_E^3}{h_E} \|\mathbf{g}_T \cdot \mathbf{n} - \mathbf{g}_{T,h} \cdot \mathbf{n}\|_{0,E}^2 \right)^{1/2} \\
 & \times \left(\sum_{E \in \mathcal{E}^{\text{int}}(\mathcal{T})} \frac{p_E}{h_E} \|\mathbf{v} - \mathbf{v}_h\|_{0,E}^2 + \sum_{E \in \mathcal{E}^D(\mathcal{T})} \frac{p_E}{h_E} \|\mathbf{v} - \mathbf{v}_h\|_{0,E}^2 \right. \\
 & \left. + \sum_{E \in \mathcal{E}^T(\mathcal{T})} \frac{p_E}{h_E} \|(\mathbf{v} - \mathbf{v}_h) \cdot \mathbf{n}\|_{0,E}^2 \right)^{1/2} \\
 & \lesssim \left[\left(\sum_{K \in \mathcal{T}} \eta_{J,K}^2 \right)^{1/2} + \left(\sum_{K \in \mathcal{T}} \text{osc}_{J,K}^2 \right)^{1/2} \right] \|\mathbf{v}\|_{\mathcal{T}}.
 \end{aligned}$$

To bound T_3 in the interior of the mesh, we use the Cauchy–Schwarz inequality, (25) and the shape regularity assumption on the mesh \mathcal{T} :

$$\begin{aligned}
 T_3|_{\mathcal{E}^{\text{int}}(\mathcal{T})} & \leq \left(\sum_{E \in \mathcal{E}^{\text{int}}(\mathcal{T})} \frac{h_E}{p_E} \|\boldsymbol{\sigma}(\mathbf{u}_h)\|_{0,E}^2 \right)^{1/2} \times \left(\sum_{E \in \mathcal{E}^{\text{int}}(\mathcal{T})} \frac{p_E}{h_E} \|\mathbf{v} - \mathbf{v}_h\|_{0,E}^2 \right)^{1/2} \\
 & \lesssim \left(\sum_{K \in \mathcal{T}} \eta_{F,K}^2 \right)^{1/2} \|\mathbf{v}\|_{\mathcal{T}}.
 \end{aligned}$$

In a similar way T_3 is bounded on the Neumann portion of boundary:

$$\begin{aligned}
 T_3|_{\mathcal{E}^N(\mathcal{T})} & \leq \left[\left(\sum_{E \in \mathcal{E}^N(\mathcal{T})} \frac{h_E}{p_E} \|\boldsymbol{\sigma}(\mathbf{u}_h) \cdot \mathbf{n}_K - \mathbf{g}_{N,h}\|_{0,E}^2 \right)^{1/2} \right. \\
 & \left. + \left(\sum_{E \in \mathcal{E}^N(\mathcal{T})} \frac{h_E}{p_E} \|\mathbf{g}_N - \mathbf{g}_{N,h}\|_{0,E}^2 \right)^{1/2} \right] \\
 & \times \left(\sum_{E \in \mathcal{E}^N(\mathcal{T})} \frac{p_E}{h_E} \|\mathbf{v} - \mathbf{v}_h\|_{0,E}^2 \right)^{1/2} \\
 & \lesssim \left[\left(\sum_{K \in \mathcal{T}} \eta_{F,K}^2 \right)^{1/2} + \left(\sum_{K \in \mathcal{T}} \text{osc}_{F,K}^2 \right)^{1/2} \right] \|\mathbf{v}\|_{\mathcal{T}}.
 \end{aligned}$$

On the Dirichlet portion of boundary, the term T_3 is null since $\mathbf{v} = \mathbf{0}$ on Γ_D :

$$\begin{aligned}
 T_3|_{\mathcal{E}^D(\mathcal{T})} & = - \sum_{E \in \mathcal{E}^D(\mathcal{T})} \int_E \boldsymbol{\sigma}(\mathbf{u}_h) \cdot \mathbf{n}_K \cdot (\mathbf{v} - \mathbf{v}_h) \, ds - \sum_{E \in \mathcal{E}^D(\mathcal{T})} \int_E \boldsymbol{\sigma}(\mathbf{u}_h) \cdot \mathbf{n}_K \cdot \mathbf{v}_h \, ds \\
 & = - \sum_{E \in \mathcal{E}^D(\mathcal{T})} \int_E \boldsymbol{\sigma}(\mathbf{u}_h) \cdot \mathbf{n}_K \cdot \mathbf{v} \, ds = 0.
 \end{aligned}$$

On the traction portion of boundary we use $\mathbf{v} \cdot \mathbf{n} = \mathbf{0}$ to bound T_3 :

$$\begin{aligned}
 T_3|_{\mathcal{E}^T(\mathcal{T})} & = - \sum_{E \in \mathcal{E}^T(\mathcal{T})} \int_E \boldsymbol{\sigma}(\mathbf{u}_h) \cdot \mathbf{n}_K \cdot (\mathbf{v} - \mathbf{v}_h) \, ds - \sum_{E \in \mathcal{E}^T(\mathcal{T})} \int_E (\mathbf{t}(\mathbf{u}_h) \cdot \mathbf{n})(\mathbf{v}_h \cdot \mathbf{n}) \, ds \\
 & = - \sum_{E \in \mathcal{E}^T(\mathcal{T})} \int_E \boldsymbol{\sigma}(\mathbf{u}_h) \cdot \mathbf{n}_K \cdot \mathbf{n}_{\parallel} (\mathbf{v} - \mathbf{v}_h) \cdot \mathbf{n}_{\parallel} \, ds \\
 & \quad - \sum_{E \in \mathcal{E}^T(\mathcal{T})} \int_E \boldsymbol{\sigma}(\mathbf{u}_h) \cdot \mathbf{n}_K \cdot \mathbf{n} (\mathbf{v} - \mathbf{v}_h) \cdot \mathbf{n} \, ds \\
 & \quad - \sum_{E \in \mathcal{E}^T(\mathcal{T})} \int_E (\mathbf{t}(\mathbf{u}_h) \cdot \mathbf{n})(\mathbf{v}_h \cdot \mathbf{n}) \, ds \\
 & = - \sum_{E \in \mathcal{E}^T(\mathcal{T})} \int_E \boldsymbol{\sigma}(\mathbf{u}_h) \cdot \mathbf{n}_K \cdot \mathbf{n}_{\parallel} (\mathbf{v} - \mathbf{v}_h) \cdot \mathbf{n}_{\parallel} \, ds \\
 & \leq \left(\sum_{E \in \mathcal{E}^T(\mathcal{T})} \frac{h_E}{p_E} \|\boldsymbol{\sigma}(\mathbf{u}_h) \cdot \mathbf{n}_K \cdot \mathbf{n}_{\parallel}\|_{0,E}^2 \right)^{1/2} \times \left(\sum_{E \in \mathcal{E}^T(\mathcal{T})} \frac{p_E}{h_E} \|\mathbf{v} - \mathbf{v}_h\|_{0,E}^2 \right)^{1/2} \\
 & \lesssim \left(\sum_{K \in \mathcal{T}} \eta_{F,K}^2 \right)^{1/2} \|\mathbf{v}\|_{\mathcal{T}}.
 \end{aligned}$$

To bound T_4 in the interior of the mesh, we use (4), the Cauchy–Schwarz inequality, the standard hp -version of the trace inequality [24] and the shape regularity assumption on the mesh \mathcal{T} :

$$\begin{aligned} T_4|_{\mathcal{E}^{\text{int}}(\mathcal{T})} &\lesssim \left(\sum_{E \in \mathcal{E}^{\text{int}}(\mathcal{T})} \frac{\gamma^2 p_E^2}{h_E} \|[\mathbf{u}_h]\|_{0,E}^2 \right)^{1/2} \times \left(\sum_{E \in \mathcal{E}^{\text{int}}(\mathcal{T})} \frac{h_E}{p_E^2} \| \{\nabla \mathbf{v}_h\} \|_{0,E}^2 \right)^{1/2} \\ &\lesssim \left(\sum_{K \in \mathcal{T}} \eta_{j,K}^2 \right)^{1/2} \| |\mathbf{v}| \|_{\mathcal{T}}, \end{aligned}$$

where in the last step we used (24):

$$\| \nabla \mathbf{v}_h \|_{0,K}^2 \lesssim \| \nabla (\mathbf{v} - \mathbf{v}_h) \|_{0,K}^2 + \| \nabla \mathbf{v} \|_{0,K}^2 \lesssim \| \nabla \mathbf{v} \|_{0,K}^2.$$

In a similar way T_4 is bounded on the Dirichlet portion of boundary:

$$\begin{aligned} T_4|_{\mathcal{E}^{\text{D}}(\mathcal{T})} &\lesssim \left[\left(\sum_{E \in \mathcal{E}^{\text{D}}(\mathcal{T})} \frac{\gamma^2 p_E^2}{h_E} \| \mathbf{u}_h - \mathbf{g}_{D,h} \|_{0,E}^2 \right)^{1/2} \right. \\ &\quad \left. + \sum_{E \in \mathcal{E}^{\text{D}}(\mathcal{T})} \frac{\gamma^2 p_E^2}{h_E} \| \mathbf{g}_D - \mathbf{g}_{D,h} \|_{0,E}^2 \right]^{1/2} \\ &\quad \times \left(\sum_{E \in \mathcal{E}^{\text{D}}(\mathcal{T})} \frac{h_E}{p_E^2} \| \nabla \mathbf{v}_h \|_{0,E}^2 \right)^{1/2} \\ &\lesssim \left[\left(\sum_{K \in \mathcal{T}} \eta_{j,K}^2 \right)^{1/2} + \left(\sum_{K \in \mathcal{T}} \text{osc}_{j,K}^2 \right)^{1/2} \right] \| |\mathbf{v}| \|_{\mathcal{T}}. \end{aligned}$$

In a similar way T_4 is bounded on the traction portion of boundary:

$$\begin{aligned} T_4|_{\mathcal{E}^{\text{T}}(\mathcal{T})} &\lesssim \left[\left(\sum_{E \in \mathcal{E}^{\text{T}}(\mathcal{T})} \frac{\gamma^2 p_E^2}{h_E} \| \mathbf{u}_h \cdot \mathbf{n} - \mathbf{g}_{T,h} \cdot \mathbf{n} \|_{0,E}^2 \right)^{1/2} \right. \\ &\quad \left. + \left(\sum_{E \in \mathcal{E}^{\text{T}}(\mathcal{T})} \frac{\gamma^2 p_E^2}{h_E} \| \mathbf{g}_T \cdot \mathbf{n} - \mathbf{g}_{T,h} \cdot \mathbf{n} \|_{0,E}^2 \right)^{1/2} \right] \\ &\quad \times \left(\sum_{E \in \mathcal{E}^{\text{T}}(\mathcal{T})} \frac{h_E}{p_E^2} \| \nabla \mathbf{v}_h \cdot \mathbf{n} \|_{0,E}^2 \right)^{1/2} \\ &\lesssim \left[\left(\sum_{K \in \mathcal{T}} \eta_{j,K}^2 \right)^{1/2} + \left(\sum_{K \in \mathcal{T}} \text{osc}_{j,K}^2 \right)^{1/2} \right] \| |\mathbf{v}| \|_{\mathcal{T}}. \end{aligned}$$

The statement of the lemma is a consequence of all the above bounds. \square

The upper bound for (32) comes from the application of Lemma 3, (33) and (36), i.e.

$$\| |\tilde{\mathbf{u}} - I_{hp} \tilde{\mathbf{u}} - \mathbf{u}_h^c \|_{\mathcal{T}} \lesssim (\eta_{\text{err}} + \text{osc}) \| |\mathbf{v}| \|_{\mathcal{T}}. \quad (39)$$

Finally the proof of Theorem 6.1 is achieved by constructing an upper bound of (27) using (28), Lemma 2 and (39).

7. Efficiency of the error estimator

In this section we prove the efficiency of the error estimator exploiting the properties of bubble functions as in [8,25–27]. The efficiency result cannot be shown uniformly in the polynomial degree since inverse estimates optimal in the polynomial degree are not currently available.

The efficiency result states that it is possible to construct an upper bound for the error estimator using the error in the DG norm. This, together with the reliability result, establishes that the error in the DG norm and the error estimator are linearly proportional quantities up to the oscillation terms that are considered of higher order. In other words we have that the error estimator cannot be “too far away” from the real value of the error.

For an element K the bubble function ψ_K is positive real valued function with compact support contained in K and bounded by 1 in the L^∞ norm. Similarly, for an edge E we define the bubble function ψ_E as a positive real valued function with compact support contained in ΔE , where ΔE is the union of the elements with an intersection with E of dimension 1, and bounded by 1 in the L^∞ norm. In [27] the explicit definitions of ψ_K and ψ_E for the 2D case can be found: denoting by $\lambda_{K,i}$ with $i = 1, 2, 3$ the barycentric coordinate of the vertex i of K

$$\psi_K = \begin{cases} 27\lambda_{K,1}\lambda_{K,2}\lambda_{K,3} & \text{in } K \\ 0 & \text{in } \Omega/K. \end{cases}$$

Denoting with $i = 1, 2$ the vertices of E and assuming they are not hanging nodes and with $\lambda_{K^+,i}$ and $\lambda_{K^-,i}$ the corresponding barycentric coordinates for the elements K^+ and K^- forming ΔE ,

$$\psi_E = \begin{cases} 4\lambda_{K^+,1}\lambda_{K^+,2} & \text{in } K^+ \\ 4\lambda_{K^-,1}\lambda_{K^-,2} & \text{in } K^- \\ 0 & \text{in } \Omega/\Delta E. \end{cases}$$

For edges touching hanging nodes, the construction using an auxiliary mesh presented in [28] can be used. The construction is very technical and for brevity it is not reported in here.

Lemma 4. *Bubble functions can be constructed such that the following results hold for any element $K \in \mathcal{T}$, for any edge $E \in \mathcal{E}(\mathcal{T})$ and any $\mathbf{v} \in V_p(\mathcal{T})$*

$$\|\mathbf{v}\|_{0,K} \lesssim \|\psi_K^{1/2}\mathbf{v}\|_{0,K}, \tag{40}$$

$$\|\nabla(\psi_K\mathbf{v})\|_{0,K} \lesssim h_K^{-1}\|\mathbf{v}\|_{0,K}, \tag{41}$$

$$\|\mathbf{v}\|_{0,E} \lesssim \|\psi_E^{1/2}\mathbf{v}\|_{0,E}, \tag{42}$$

$$\|\nabla(\psi_E\mathbf{v})\|_{0,\Delta E} \lesssim h_K^{-1/2}\|\mathbf{v}\|_{0,E}, \tag{43}$$

$$\|\psi_E\mathbf{v}\|_{0,\Delta E} \lesssim h_K^{1/2}\|\mathbf{v}\|_{0,E}. \tag{44}$$

See Lemma 3.3 in [27] for the proof. Next we have the efficiency result:

Theorem 7.1. *Let \mathbf{u} the exact solution and \mathbf{u}_h the computed solution, we have that*

$$\eta_{\text{err}} \leq C(\|\mathbf{u} - \mathbf{u}_h\|_{\mathcal{T}} + \text{osc}),$$

where C is a positive constant independent of the mesh nor the order of the elements used.

Proof. Starting with $\eta_{J,K}$, we have that $[\![\mathbf{u}]\!] = 0$ on all interior faces, then

$$\sum_{E \in \mathcal{E}^{\text{int}}(K)} \frac{\gamma^2 p_E^3}{h_E} \|\![\mathbf{u}_h]\!\|_{0,E}^2 = \sum_{E \in \mathcal{E}^{\text{int}}(K)} \frac{\gamma^2 p_E^3}{h_E} \|\![\mathbf{u}_h - \mathbf{u}]\!\|_{0,E}^2 \lesssim p_E \|\mathbf{u} - \mathbf{u}_h\|_{\omega_K},$$

where $\|\cdot\|_{\omega_K}$ is the DG norm computed on all the elements intersecting K and its faces. Similarly $\mathbf{u} = \mathbf{g}_D$ on Γ_D and $\mathbf{u} \cdot \mathbf{n} = \mathbf{g}_T \cdot \mathbf{n}$ on Γ_T , so we have

$$\begin{aligned} & \sum_{E \in \mathcal{E}^D(K)} \frac{\gamma^2 p_E^3}{h_E} \|\mathbf{u}_h - \mathbf{g}_{D,h}\|_{0,E}^2 + \sum_{E \in \mathcal{E}^T(K)} \frac{\gamma^2 p_E^3}{h_E} \|\mathbf{u}_h \cdot \mathbf{n} - \mathbf{g}_{T,h} \cdot \mathbf{n}\|_{0,E}^2 \\ & \lesssim \sum_{E \in \mathcal{E}^D(K)} \frac{\gamma^2 p_E^3}{h_E} \|\mathbf{u}_h - \mathbf{u}\|_{0,E}^2 + \sum_{E \in \mathcal{E}^T(K)} \frac{\gamma^2 p_E^3}{h_E} \|\mathbf{u}_h \cdot \mathbf{n} - \mathbf{u} \cdot \mathbf{n}\|_{0,E}^2 \\ & \quad + \sum_{E \in \mathcal{E}^D(K)} \frac{\gamma^2 p_E^3}{h_E} \|\mathbf{g}_D - \mathbf{g}_{D,h}\|_{0,E}^2 + \sum_{E \in \mathcal{E}^T(K)} \frac{\gamma^2 p_E^3}{h_E} \|\mathbf{g}_T \cdot \mathbf{n} - \mathbf{g}_{T,h} \cdot \mathbf{n}\|_{0,E}^2 \\ & \lesssim p_E \|\mathbf{u} - \mathbf{u}_h\|_{\omega_K} + \left(\sum_{K \in \omega_K} \text{osc}_{J,K}^2 \right)^{1/2}. \end{aligned}$$

Moving on to the term $\eta_{R,K}$ and assuming that it is non-zero, we define $\mathbf{w} := \frac{h_K^2}{p_K^2} (\mathbf{f}_h + \nabla \cdot \boldsymbol{\sigma}(\mathbf{u}_h)) \psi_K$, then using (40) we have

$$\eta_{R,K}^2 \lesssim \int_K (\mathbf{f}_h + \nabla \cdot \boldsymbol{\sigma}(\mathbf{u}_h)) \cdot \mathbf{w} \, dx = \int_K (-\nabla \cdot \boldsymbol{\sigma}(\mathbf{u}) + \nabla \cdot \boldsymbol{\sigma}(\mathbf{u}_h)) \cdot \mathbf{w} \, dx + \int_K (\mathbf{f}_h - \mathbf{f}) \cdot \mathbf{w} \, dx.$$

Then applying integration by parts and using the fact that $\mathbf{w}|_{\partial K} = 0$ we have

$$\eta_{R,K}^2 \lesssim \|\boldsymbol{\sigma}(\mathbf{u}) - \boldsymbol{\sigma}(\mathbf{u}_h)\|_{0,K} \|\nabla \mathbf{w}\|_{0,K} + \|\mathbf{f} - \mathbf{f}_h\|_{0,K} \|\mathbf{w}\|_{0,K}.$$

Then using (4), (41) and the fact that $\psi_K \lesssim 1$, we obtain

$$\begin{aligned} \eta_{R,K}^2 & \lesssim \|\mathbf{u} - \mathbf{u}_h\|_K \|\nabla \mathbf{w}\|_{0,K} + \|\mathbf{f} - \mathbf{f}_h\|_{0,K} \|\mathbf{w}\|_{0,K} \\ & \lesssim h_K^{-1} \|\mathbf{u} - \mathbf{u}_h\|_K \frac{h_K^2}{p_K^2} \|\mathbf{f}_h + \nabla \cdot \boldsymbol{\sigma}(\mathbf{u}_h)\|_{0,K} + \frac{h_K^2}{p_K^2} \|\mathbf{f} - \mathbf{f}_h\|_{0,K} \|\mathbf{f}_h + \nabla \cdot \boldsymbol{\sigma}(\mathbf{u}_h)\|_{0,K}. \end{aligned}$$

Finally dividing both sides by $\frac{h_K}{p_K} \|\mathbf{f}_h + \nabla \cdot \boldsymbol{\sigma}(\mathbf{u}_h)\|_{0,K}$ we obtain

$$\eta_{R,K} \lesssim p_K^{-1} \|\mathbf{u} - \mathbf{u}_h\|_K + \frac{h_K}{p_K} \|\mathbf{f} - \mathbf{f}_h\|_{0,K}. \tag{45}$$

In case that $\eta_{R,K} = 0$, then any non-negative quantity can be used to bound it and in particular (45) holds.

For the term $\eta_{F,K}$ we have that $\llbracket \boldsymbol{\sigma}(\mathbf{u}) \rrbracket = 0$ in the interior of the mesh, then defining $\mathbf{w} := \frac{h_E}{p_E} \llbracket \boldsymbol{\sigma}(\mathbf{u}_h) \rrbracket \psi_E$ we have using (42)

$$\frac{h_E}{p_E} \|\llbracket \boldsymbol{\sigma}(\mathbf{u}_h) \rrbracket\|_{0,E}^2 \lesssim \int_E \llbracket \boldsymbol{\sigma}(\mathbf{u}_h) \rrbracket \cdot \mathbf{w} \, ds = \int_E \llbracket \boldsymbol{\sigma}(\mathbf{u}_h) - \boldsymbol{\sigma}(\mathbf{u}) \rrbracket \cdot \mathbf{w} \, ds.$$

Then assuming that $\frac{h_E}{p_E} \|\llbracket \boldsymbol{\sigma}(\mathbf{u}_h) \rrbracket\|_{0,E}^2 > 0$ and integrating by parts:

$$\frac{h_E}{p_E} \|\llbracket \boldsymbol{\sigma}(\mathbf{u}_h) \rrbracket\|_{0,E}^2 \lesssim \int_{\Delta E} \nabla \cdot (\boldsymbol{\sigma}(\mathbf{u}_h) - \boldsymbol{\sigma}(\mathbf{u})) \cdot \mathbf{w} + (\boldsymbol{\sigma}(\mathbf{u}_h) - \boldsymbol{\sigma}(\mathbf{u})) \cdot \nabla \mathbf{w} \, dx.$$

The second term can be bounded using (4) and (43)

$$\begin{aligned} \int_{\Delta E} (\boldsymbol{\sigma}(\mathbf{u}_h) - \boldsymbol{\sigma}(\mathbf{u})) \cdot \nabla \mathbf{w} \, dx &\lesssim \|\mathbf{u} - \mathbf{u}_h\|_{\Delta E} \|\nabla \mathbf{w}\|_{0,\Delta E} \\ &\lesssim \|\mathbf{u} - \mathbf{u}_h\|_{\Delta E} h_E^{-1/2} \frac{h_E}{p_E} \|\llbracket \boldsymbol{\sigma}(\mathbf{u}_h) \rrbracket\|_{0,E} \\ &= \|\mathbf{u} - \mathbf{u}_h\|_{\Delta E} p_E^{-1/2} \left\| \frac{h_E^{-1/2}}{p_E^{-1/2}} \llbracket \boldsymbol{\sigma}(\mathbf{u}_h) \rrbracket \right\|_{0,E} \end{aligned}$$

To bound the first term we define $\tilde{\mathbf{w}} = \mathbf{w} \psi_{\Delta K}$, with $\psi_{\Delta K} = \sum_{K \in \Delta E} \psi_K$. Then using (40) we have

$$\int_{\Delta E} \nabla \cdot (\boldsymbol{\sigma}(\mathbf{u}_h) - \boldsymbol{\sigma}(\mathbf{u})) \cdot \mathbf{w} \, dx \lesssim \int_{\Delta E} \nabla \cdot (\boldsymbol{\sigma}(\mathbf{u}_h) - \boldsymbol{\sigma}(\mathbf{u})) \cdot \tilde{\mathbf{w}} \, dx$$

Then using integration by parts and using (41) and (44):

$$\begin{aligned} \int_{\Delta E} \nabla \cdot (\boldsymbol{\sigma}(\mathbf{u}_h) - \boldsymbol{\sigma}(\mathbf{u})) \cdot \tilde{\mathbf{w}} \, dx &\lesssim h_k^{-1} h_E^{1/2} \|\mathbf{u} - \mathbf{u}_h\|_{\Delta E} \frac{h_E}{p_E} \|\llbracket \boldsymbol{\sigma}(\mathbf{u}_h) \rrbracket\|_{0,E} \\ &= p_E^{-1/2} \|\mathbf{u} - \mathbf{u}_h\|_{\Delta E} \frac{h_E}{p_E} \|\llbracket \boldsymbol{\sigma}(\mathbf{u}_h) \rrbracket\|_{0,E}. \end{aligned}$$

Putting everything together we have

$$\left\{ \frac{h_E}{p_E} \|\llbracket \boldsymbol{\sigma}(\mathbf{u}_h) \rrbracket\|_{0,E}^2 \right\}^{1/2} \lesssim p_E^{-1/2} \|\mathbf{u} - \mathbf{u}_h\|_{\Delta E} \tag{46}$$

In case that $\frac{h_E}{p_E} \|\llbracket \boldsymbol{\sigma}(\mathbf{u}_h) \rrbracket\|_{0,E} = 0$, then any non-negative quantity can be used to bound it and in particular (46) holds.

On Γ_N we define $\mathbf{w} := \frac{h_E}{p_E} (\boldsymbol{\sigma}(\mathbf{u}_h) \cdot \mathbf{n} - \mathbf{g}_{N,h}) \psi_E$ we use (42):

$$\frac{h_E}{p_E} \|(\boldsymbol{\sigma}(\mathbf{u}_h) \cdot \mathbf{n} - \mathbf{g}_{N,h})\|_{E,0} \lesssim \int_E (\boldsymbol{\sigma}(\mathbf{u}_h) \cdot \mathbf{n} - \mathbf{g}_N) \cdot \mathbf{w} \, ds + \int_E (\mathbf{g}_N - \mathbf{g}_{N,h}) \cdot \mathbf{w} \, ds. \tag{47}$$

Assuming that $\frac{h_E}{p_E} \|(\boldsymbol{\sigma}(\mathbf{u}_h) \cdot \mathbf{n} - \mathbf{g}_{N,h})\|_{E,0} > 0$, the first integral in (47) can be bounded noticing that $\boldsymbol{\sigma}(\mathbf{u}) \cdot \mathbf{n} = \mathbf{g}_N$ and using integration by parts as for $\eta_{F,K}$ on the interior faces:

$$\int_E (\boldsymbol{\sigma}(\mathbf{u}_h) \cdot \mathbf{n} - \mathbf{g}_N) \cdot \mathbf{w} \, ds \lesssim p_E^{-1/2} \|\mathbf{u} - \mathbf{u}_h\|_{\Delta E} \left\| \frac{h_E^{-1/2}}{p_E^{-1/2}} (\boldsymbol{\sigma}(\mathbf{u}_h) \cdot \mathbf{n} - \mathbf{g}_{N,h}) \right\|_{E,0}.$$

The second integral can be bounded using $\psi_E \approx 1$

$$\begin{aligned} \int_E (\mathbf{g}_N - \mathbf{g}_{N,h}) \cdot \mathbf{w} \, ds &\lesssim \int_E (\mathbf{g}_N - \mathbf{g}_{N,h}) \cdot \frac{h_E}{p_E} (\boldsymbol{\sigma}(\mathbf{u}_h) \cdot \mathbf{n} - \mathbf{g}_{N,h}) \, ds \\ &\leq \left\| \frac{h_E^{-1/2}}{p_E^{-1/2}} (\mathbf{g}_N - \mathbf{g}_{N,h}) \right\|_{E,0} \left\| \frac{h_E^{-1/2}}{p_E^{-1/2}} (\boldsymbol{\sigma}(\mathbf{u}_h) \cdot \mathbf{n} - \mathbf{g}_{N,h}) \right\|_{E,0} \end{aligned}$$

This leads to:

$$\left(\frac{h_E}{p_E} \|(\boldsymbol{\sigma}(\mathbf{u}_h) \cdot \mathbf{n} - \mathbf{g}_{N,h})\|_{E,0} \right)^{1/2} \lesssim p_E^{-1/2} \|\mathbf{u} - \mathbf{u}_h\|_{\Delta E} + \left(\sum_{K \in \mathcal{T}} \text{osc}_{F,K}^2 \right)^{1/2} \tag{48}$$

In case that $\frac{h_E}{p_E} \|(\boldsymbol{\sigma}(\mathbf{u}_h) \cdot \mathbf{n} - \mathbf{g}_{N,h})\|_{E,0} = 0$, then any non-negative quantity can be used to bound it and in particular (48) holds.

Finally to bound the term on Γ_T we define $\mathbf{w} := \frac{h_E}{p_E} \mathbf{t}(\mathbf{u}_h) \cdot \mathbf{n}_{\parallel} \psi_E$ and we proceed in the same way as before using the fact that $\mathbf{t}(\mathbf{u}) \cdot \mathbf{n}_{\parallel} = 0$ and applying integration by parts. This leads to the bound

$$\left\{ \frac{h_E}{p_E} \|\mathbf{t}(\mathbf{u}_h) \cdot \mathbf{n}_{\parallel}\|_{E,0} \right\}^{1/2} \lesssim p_E^{-1/2} \|\mathbf{u} - \mathbf{u}_h\|_{\Delta E}$$

Putting together the bounds for all terms, the proof of the theorem is concluded. \square

8. Numerical examples

In this section the *a posteriori* error estimator, (19), for smooth and non-smooth problems will be shown to be efficient, reliable, and with an exponential performance in the error estimate value (19) and the error in the DG norm (13).

The finite elements used in the simulations are arbitrary high order triangular elements as defined in [29]. The *hp*-adaptive strategy used here was originally proposed in [30] and was shown to be proficient for finite elements in [31]. The elements are chosen for either *h* or *p* refinement using Algorithm 1. The marking strategy in Algorithm 1 uses two threshold values δ_1 and δ_2 , with $\delta_2 \geq \delta_1$, to determine what elements to refine in *h* and what elements in *p*. The assumption behind the marking strategy is that the elements associated to the highest values of the error estimator are localized where the solution is less smooth and therefore they have to be refined in *h*. In view of this, all the elements satisfying $\eta_K^2 > \delta_2 \eta_{\max}^2$, where $\eta_{\max}^2 = \max_{K \in \mathcal{T}} \eta_K^2$, are marked for *h*-refinement and all elements satisfying $\delta_2 \eta_{\max}^2 \geq \eta_K^2 > \delta_1 \eta_{\max}^2$ are marked for *p*-refinement. The remaining elements are not marked for refinement at all. To perform *h* adaptivity only, set $\delta_2 = \delta_1 \neq 0$ and to adaptively refine in *p* only set $\delta_2 = 1$ and $\delta_1 \neq 0$. To adaptively refine in *hp* simply ensure $\delta_2 > \delta_1$. To uniformly refine in *h* set $\delta_2 = \delta_1 = 0$ and to uniformly refine in *p* set $\delta_2 = 1$ and $\delta_1 = 0$. All adaptive strategies are halted once the number of degrees of freedom (ndof) of the linear system exceeds 10^4 .

To uniformly refine in *h* set $\delta_2 = \delta_1 = 0$ and to uniformly refine in *p* set $\delta_2 = 1$ and $\delta_1 = 0$. The strategy assumes that if $\eta_K^2 > \delta_2 \eta_{\max}^2$, where $\eta_{\max}^2 = \max_{K \in \mathcal{T}} \eta_K^2$, the real solution in element *K* is non-smooth and so *h*-refinement is necessary. If $\delta_2 \eta_{\max}^2 \geq \eta_K^2 \geq \delta_1 \eta_{\max}^2$ the real solution is assumed smooth however the polynomial order is too low to capture the real solution to a sufficient accuracy. Many adaptive strategies exist, a review is provided in [30], this strategy was chosen as it was the simplest to facilitate and demonstrate the efficacy of the error estimator. To perform *h* adaptivity only, set $\delta_2 = \delta_1 \neq 0$ and to adaptively refine in *p* set $\delta_2 = 1$ and $\delta_1 \neq 0$. To adaptively refine in *hp* simply ensure $\delta_2 \neq \delta_1$. All adaptive strategies are halted once the number of degrees of freedom (ndof) of the linear system exceeds 10^4 .

Algorithm 1. *hp*-refinement strategy: for parameters δ_1, δ_2 with $1 \geq \delta_2 \geq \delta_1 \geq 0$.

- 1) Compute the maximum error $\eta_{\max}^2 = \max_{K \in \mathcal{T}} \eta_K^2$.
 - 2) Identify the set of elements to refine in *p*: $\mathcal{T}_{p_ref} = \{K \in \mathcal{T} | \delta_2 \eta_{\max}^2 \geq \eta_K^2 > \delta_1 \eta_{\max}^2\}$.
 - 3) Increase p_K by one for $K \in \mathcal{T}_{p_ref}$.
 - 4) Identify the set of elements to refine in *h*: $\mathcal{T}_{h_ref} = \{K \in \mathcal{T} | \eta_K^2 > \delta_2 \eta_{\max}^2\}$.
 - 4) Identify any elements $K \in \mathcal{T} \cap \mathcal{T}'$, where \mathcal{T}' is the refined mesh, that will have more than one hanging node on a face and add to \mathcal{T}_{h_ref} .
 - 5) *h* refine all elements $K \in \mathcal{T}_{h_ref}$ to create the new mesh \mathcal{T}' .
 - 7) Ensure for every pair of neighbours $K, K' \in \mathcal{T}'$ that (8) is satisfied, otherwise add K' , where $p_{K'} < p_K$, to the set \mathcal{T}'_{p_ref} .
 - 9) Increase p_K by one for $K \in \mathcal{T}'_{p_ref}$.
-

8.1. Smooth solution problem

We consider a small strain linear elastic problem on $(x, y) \in \Omega = (0, 1)^2$, where *x* and *y* are in metres. The problem acts in plane strain with Young's modulus $E_Y = \frac{5}{2}$ Pa, and a Poisson's ratio $\nu = \frac{1}{4}$. The right-hand side **f** of problem (1) is chosen such that the exact analytical solution is smooth over the entire domain,

$$\mathbf{u} = \left\{ \begin{array}{l} \sin(2\pi x) \sin(2\pi y) \\ \sin(2\pi x) \sin(2\pi y) \end{array} \right\}.$$

The initial mesh is conforming and is constructed from 32 elements with $p_K = 3$ for all $K \in \mathcal{T}$. The right-hand side is applied to the problem as a body force and with $\mathbf{g}_D = \mathbf{0}$ on Γ_D where $\partial\Omega = \Gamma_D$. The *hp*-adaptive strategy uses $\delta_2 = 0.7$ and

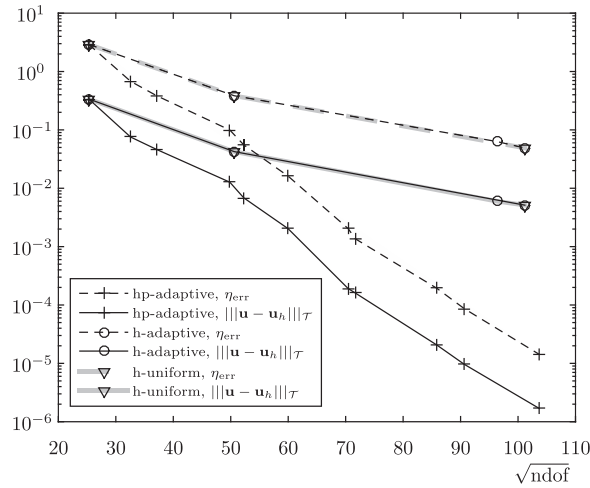


Fig. 1. Square domain – performance of the error estimator, η_{err} (19), and the error in the DG norm $\|u - u_h\|_{\mathcal{T}}$ against \sqrt{ndof} for different adaptive strategies.

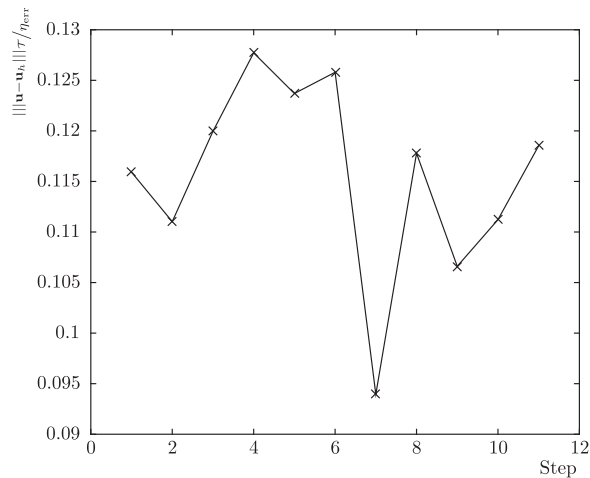


Fig. 2. Square domain – performance of $\frac{\|u - u_h\|_{\mathcal{T}}}{\eta_{err}}$, Theorem 6.1, against the refinement step for the hp-adaptive strategy.

$\delta_1 = 0.07$, from [31]. As noted in [31], since the solution is regular over the entire domain, and therefore smooth, adaptive p -refinement would produce the greatest reduction in error per unit cost in degrees of freedom. However it is demonstrated here for linear elasticity that this hp -adaptive strategy is still capable of producing exponential convergence. Additionally for comparison, the h -adaptive strategy uses $\delta_2 = \delta_1 = 0.07$. In Fig. 1 the error estimate value and the error in the DG norm are plotted against \sqrt{ndof} for, hp -adaptive, h -adaptive, and uniform h -refinement on a linear log scale. Fig. 1 shows only the hp -adaptive strategy to achieve exponential convergence for the DG norm and error estimate value, this is demonstrated by the (roughly) straight lines. Additionally in Fig. 2 we plot $\frac{\|u - u_h\|_{\mathcal{T}}}{\eta_{err}}$, against refinement step for the hp -refinement strategy. The variation in $\frac{\|u - u_h\|_{\mathcal{T}}}{\eta_{err}}$ is oscillatory within a small range, which supports the fact that η_{err} is efficient and reliable for smooth problems.

The hp -strategy employed here will always perform some h -refinement, unless $\delta_2 = 1$. Other hp -adaptive methods can achieve exponential convergence though p -adaptivity only, these adapt by evaluating whether the solution is locally smooth on an element by examining the decay of the element’s Legendre coefficients [32,33]. A thorough investigation is presented in [31].

8.2. L-shaped non-smooth problem

The next problem considered is a linear elastic problem on $(x, y) \in \Omega = (-0.5, 0.5)^2 / ([0, 0.5] \times [-0.5, 0])$, where x and y are in metres, acting in plane strain with $E_Y = \frac{5}{2}$ Pa and $\nu = \frac{1}{4}$. The right-hand side \mathbf{f} in (1) is chosen such that the problem

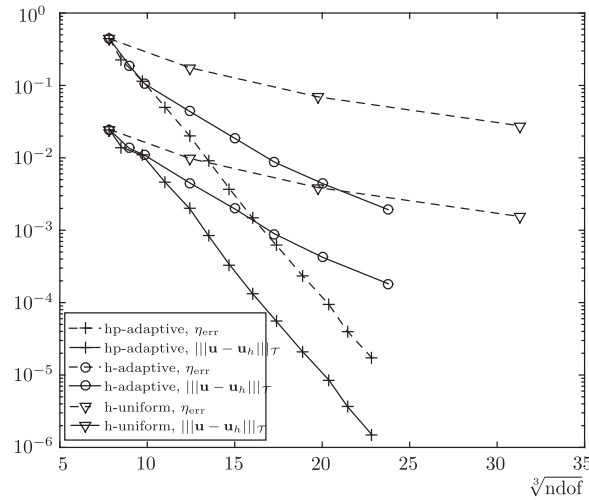


Fig. 3. L-shaped domain – performance of the error estimator, η_{err} (19), and the error in the DG norm, $\|\mathbf{u} - \mathbf{u}_h\|_{\mathcal{T}}$, against $\sqrt[3]{\text{ndof}}$ for different adaptive strategies.

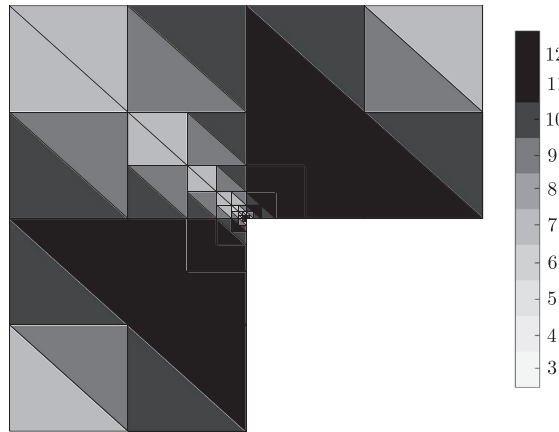


Fig. 4. L-shaped domain – element and polynomial order distribution for the L-shaped domain after the 13th hp -adaptive step.

is singular at $(x, y) = (0, 0)$,

$$\mathbf{u} = \begin{Bmatrix} (x^2 + y^2)^{\frac{2}{3}} \\ (x^2 + y^2)^{\frac{2}{3}} \end{Bmatrix}.$$

On the boundary of the problem $\partial\Omega = \Gamma_D$ we have $\mathbf{g}_D = \mathbf{u}$ on Γ_D . The initial mesh is conforming and is constructed from 6 elements with $p_K = 3$ for all $K \in \mathcal{T}$. For this problem the solution at the convex corner is non-smooth, the error estimator here is therefore likely to be higher here than in the remainder domain. As in [31] we set $\delta_2 = 0.7$ to capture the regions elements where the solution is non-smooth and perform h -refinements. $\delta_1 = 0.07$ is set to capture remain regions of the domain where the solution is smooth but not sufficiently refined. The h -adaptive strategy used $\delta_2 = \delta_1 = 0.07$. On Fig. 3 the error in the DG norm and the error estimator value are plotted against $\sqrt[3]{\text{ndof}}$. $\sqrt[3]{\text{ndof}}$ is chosen as the best known hp -strategy for finite element methods achieves an error bound for a singular problem of $\|\mathbf{u} - \mathbf{u}_h\|_{H^1(\Omega)} \leq Ce^{-b(\text{ndof})^{\frac{1}{3}}}$, see [34].

For the singular problem the hp -adaptive strategy achieves exponential convergence of the error estimator and the error in the DG norm, this is demonstrated by the roughly straight line on the linear-log plot. Additionally, Fig. 4 shows the hp -strategy to refine in h around the singularity and p in regions where the solution is smooth, consistent with [31,35]. Last the oscillations in $\frac{\|\mathbf{u} - \mathbf{u}_h\|_{\mathcal{T}}}{\eta_{\text{err}}}$, Fig. 5, show the error estimator to be efficient and reliable for singular problems.

8.3. Crack in a plate problem

Last we consider a problem with a stronger singularity, a crack in a plate acting in plane strain with $E_Y = \frac{5}{2}$ Pa and $\nu = \frac{1}{4}$. The domain of the problem is described as $(x, y) \in \Omega = ((0, 1.5) \times (-1.5, -1.5)) / ([0, 0.5] \times \{0\})$, where x and y are

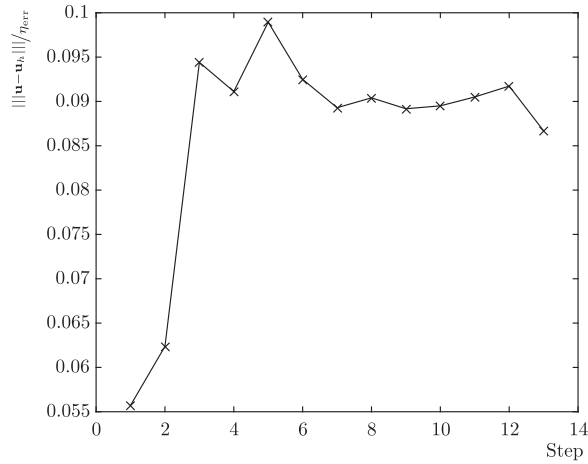


Fig. 5. L-shaped domain – performance of $\frac{\|u-u_h\|_r}{\eta_{err}}$, Theorem 6.1, against the refinement step for the hp -adaptive strategy.

in metres, with the crack tip at the point $(x, y) = (0.5, 0)$. The boundary of the problem is defined as $\partial\Omega = \Gamma_N \cup \Gamma_D \cup \Gamma_T$, where $\Gamma_N = \Gamma_{N_1} \cup \Gamma_{N_2}$, and

$$\sigma(\mathbf{u}) \cdot \mathbf{n} = p_r \cdot \mathbf{n} \text{ on } \Gamma_{N_1} = ([0, 0.5] \times \{-1.5\})$$

$$\mathbf{u} = \mathbf{0} \text{ on } \Gamma_D = ([0, 0.5] \times \{1.5\})$$

$$\mathbf{u} \cdot \mathbf{n} = 0 \text{ on } \Gamma_T = (\{0.5\} \times [-1.5, 1.5])$$

$$\mathbf{t}(\mathbf{u}) \cdot \mathbf{n}_{\parallel} = 0 \text{ on } \Gamma_T$$

$$\sigma(\mathbf{u}) \cdot \mathbf{n} = \mathbf{0} \text{ on } \Gamma_{N_2} = \partial\Omega \setminus (\Gamma_{N_1} \cup \Gamma_D \cup \Gamma_T)$$

and $p_r = 1$ Pa is an applied pressure. This is a mixed mode crack problem with jumps in both components of \mathbf{u} across the crack faces, represented by the line $([0, 0.5] \times \{0\})$ in metres [36]. The near crack tip displacement field was first derived by Irwin [36]. It is presented here in polar coordinates (r, θ) , where the crack tip is the origin,

$$\mathbf{u} = \frac{(1 + \nu)}{E} \sqrt{\frac{r}{2\pi}} \begin{Bmatrix} K_I \cos\left(\frac{\theta}{2}\right)[\kappa - 1 + 2 \sin^2\left(\frac{\theta}{2}\right)] + K_{II} \sin\left(\frac{\theta}{2}\right)[\kappa + 1 + 2 \cos^2\left(\frac{\theta}{2}\right)] \\ K_I \sin\left(\frac{\theta}{2}\right)[\kappa + 1 - 2 \cos^2\left(\frac{\theta}{2}\right)] - K_{II} \cos\left(\frac{\theta}{2}\right)[\kappa - 1 - 2 \sin^2\left(\frac{\theta}{2}\right)] \end{Bmatrix}, \tag{49}$$

and $\kappa = (3 - 4\nu)$, $\frac{r}{a} \ll 1$, with $a = 0.5$ m as length of the crack and K_I and K_{II} as stress intensity factors which are depending on the loading, geometry and boundary conditions of the problem. A displacement solution does not exist for the entire domain, however the stress singularity at the crack tip is clearly stronger than that found in Section 8.2.

To model the problem, the initial mesh is conforming and is constructed from 6 elements with $p_K = 3$ for all $K \in \mathcal{T}$. The hp -adaptive strategy used $\delta_2 = 0.7$ and $\delta_1 = 0.2$, and the h -adaptive strategy used $\delta_2 = \delta_1 = 0.2$. Although $\delta_2 = 0.07$

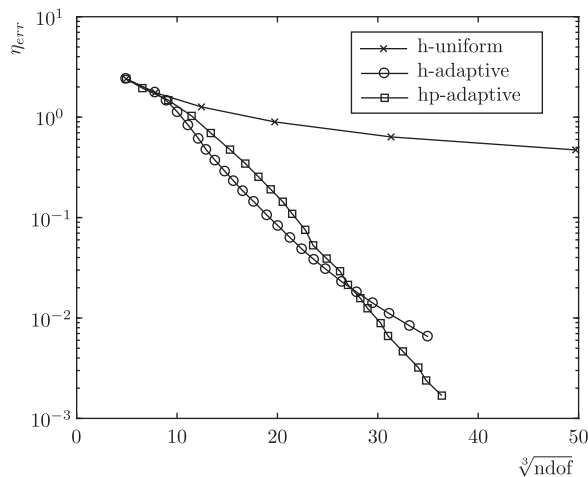


Fig. 6. Crack in a plate – performance of the error estimator for different schemes against $\sqrt[3]{\text{ndof}}$.

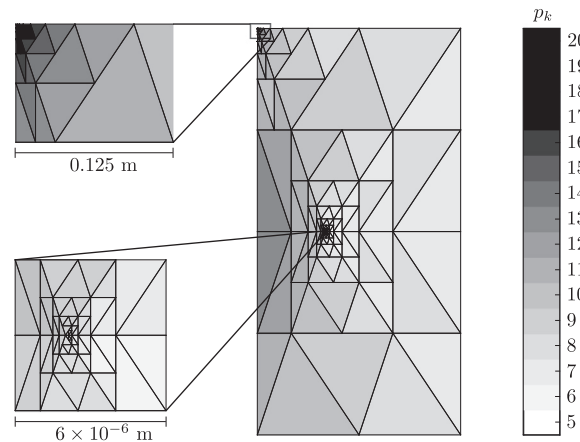


Fig. 7. Crack in a plate – element and polynomial order distribution for the plate with a crack (denoted by the white line) after the 25th hp -adaptive step. Included is a close up of the element and polynomial order distribution around the crack tip and the top left corner.

produced exponential convergence with hp -adaptivity, δ_2 was raised to 0.2 as this produced faster convergence by preventing unnecessary p -refinement in areas of the domain where the solution could be relatively well represented by low order polynomial functions.

In Fig. 6 the error estimator values are plotted against $\sqrt[3]{\text{ndof}}$.

The element and polynomial order distribution is presented in Fig. 7. The highest h -refinement levels are generated at the singular stress field at the crack tip. hp -refinement also occurs in the top-left corner of the problem where the stress field is also non-smooth, this results in relatively high error estimate values however not as high as the crack tip. For this singular problem only the hp -adaptive refinement scheme produced exponential convergence, the h -adaptive and h -uniform schemes produced only polynomial convergence.

9. Conclusions

The paper has presented, for the first time, an hp a posteriori error estimator for the symmetric interior penalty discontinuous Galerkin finite element method for linear elastic analysis. The error estimator was incorporated into an hp -adaptive finite element solver and verified against smooth and non-smooth problems with closed-form analytical solutions as well as being demonstrated on a non-smooth problem with complex boundary conditions. The hp -adaptive finite element analyses achieve exponential rates of convergence and are contrasted against uniform and adaptive h refinement.

The paper has provided a complete framework for adaptivity in the symmetric interior penalty discontinuous Galerkin finite element method for linear elastic analysis. This will allow engineers and scientists to use the method to obtain highly-accurate but efficient stress analysis results in areas where the displacement/stress solution is of paramount importance, fatigue analysis for example.

Acknowledgments

This work was supported by the Engineering and Physical Sciences Research Council grant number [EP/M507854/1]. All data created during this research are openly available at doi:10.15128/r2qn59q397h.

Supplementary material

Supplementary material associated with this article can be found, in the online version, at 10.1016/j.amc.2018.08.039.

References

- [1] M. Ainsworth, J. Oden, A posteriori error estimation in finite element analysis, *Comput. Methods Appl. Mech. Eng.* 142 (1) (1997) 1–88.
- [2] W. Reed, T. Hill, *Triangular Mesh Methods for the Neutron Transport Equation*, Technical Report LA-UR-73-479, Los Alamos Scientific Laboratory, 1973.
- [3] F. Bassi, S. Rebay, A high-order accurate discontinuous finite element method for the numerical solution of the compressible Navier–Stokes equations, *J. Comput. Phys.* 131 (1997) 267–279.
- [4] P. Castillo, B. Cockburn, I. Perugia, D. Schtzau, An a priori error analysis of the local discontinuous Galerkin method for elliptic problems, *SIAM J. Numer. Anal.* 38 (5) (2000) 1676–1706.
- [5] B. Cockburn, G. Kanschat, I. Perugia, D. Schtzau, Superconvergence of the local discontinuous Galerkin method for elliptic problems on cartesian grids, *SIAM J. Numer. Anal.* 39 (1) (2002) 264–285.
- [6] D.N. Arnold, F. Brezzi, B. Cockburn, L.D. Marini, Unified analysis of discontinuous Galerkin methods for elliptic problems, *SIAM J. Numer. Anal.* 39 (5) (2002) 1749–1779.

- [7] P. Houston, E. Süli, T.P. Wihler, A-posteriori error analysis of hp -version discontinuous Galerkin finite-element methods for second-order quasi-linear elliptic PDEs, *IMA J. Numer. Anal.* 28 (2008) 245–273.
- [8] L. Zhu, D. Schötzau, A robust a posteriori error estimate for hp -adaptive DG methods for convection–diffusion equations, *IMA J. Numer. Anal.* 31 (2010) 971–1005.
- [9] S. Giani, An a posteriori error estimator for hp -adaptive discontinuous Galerkin methods for computing band gaps in photonic crystals, *J. Comput. Appl. Math.* 236 (2012) 4810–4826.
- [10] S. Giani, D. Schötzau, L. Zhu, An a-posteriori error estimate for hp -adaptive DG methods for convection-diffusion problems on anisotropically refined meshes, *Comput. Math. Appl.* 67 (2014) 869–887.
- [11] B. Stamm, A posteriori estimates for the bubble stabilized discontinuous Galerkin method, *J. Comput. Appl. Math.* 235 (2011) 4309–4324.
- [12] G.A. Holzapfel, *Nonlinear Solid Mechanics: A Continuum Approach for Engineering*, Wiley, 2000.
- [13] B. Robert, C. Will, G. Stefano, A quasi-static discontinuous Galerkin configurational force crack propagation method for brittle materials, *Int. J. Numer. Methods Eng.* 113 (7) (2018) 1061–1080.
- [14] S. Prudhomme, E. Pascal, J. Oden, A. Romkes, Review of a Priori Error Estimation for Discontinuous Galerkin Methods, <http://citeseerx.ist.psu.edu/viewdoc/summary?doi=10.1.1.28.2750>.
- [15] I. Babuška, M. Suri, The optimal convergence rate of the p -version of the finite element method, *SIAM J. Numer. Anal.* 24 (4) (1987) 750–776.
- [16] I. Babuška, M. Suri, The $h - p$ version of the finite element method with quasiuniform meshes, *ESAIM Math. Model. Numer. Anal.* 21 (2) (1987) 199–238.
- [17] P. Houston, C. Schwab, E. Süli, Discontinuous hp -finite element methods for advection–diffusion reaction problems, *SIAM J. Numer. Anal.* 39 (6) (2002) 2133–2163.
- [18] P. Houston, D. Schötzau, T.P. Wihler, Energy norm a posteriori error estimation of hp -adaptive discontinuous Galerkin methods for elliptic problems, *Math. Models Methods Appl. Sci.* 17 (2007) 33–62.
- [19] F. Brezzi, M. Fortin, *Mixed and Hybrid Finite Element Methods*, Springer Series in Computational Mathematics, 15, Springer Verlag, 1991.
- [20] R. Adams, J. Fournier, *Sobolev Spaces, Pure and Applied Mathematics*, Elsevier Science, 2003.
- [21] R.E. Bird, W.M. Coombs, S. Giani, Supporting data: a posteriori discontinuous Galerkin error estimator for linear elasticity. URL <https://collections.durham.ac.uk/files/r2qn59q397h#445.Wz9uOhgnYpg>
- [22] J.M. Melenk, hp -interpolation of nonsmooth function and an application to hp -a posteriori error estimation, *SIAM J. Numer. Anal.* 43 (1) (2005) 127.
- [23] O. Karakashian, F. Pascal, Convergence of adaptive discontinuous Galerkin approximations of second-order elliptic problems, *SIAM J. Numer. Anal.* 45 (2) (2007) 641–665.
- [24] C. Schwab, *p - and hp -Finite Element Methods: Theory and Applications to Solid and Fluid Mechanics*, Oxford University Press, USA, 1999.
- [25] L. Zhu, S. Giani, P. Houston, D. Schoetzau, Energy norm a-posteriori error estimation for hp -adaptive discontinuous Galerkin methods for elliptic problems in three dimensions, *Math. Models Methods Appl. Sci.* 21 (2) (2011) 267–306.
- [26] S. Giani, I. Graham, Adaptive finite element methods for computing band gaps in photonic crystals, *Numer. Math.* 121 (1) (2012) 31–64.
- [27] R. Verfürth, *A Review of Posteriori Error Estimation and Adaptive Mesh Refinement Techniques*, Wiley-Teubner, 1996.
- [28] L. Zhu, Robust a Posteriori Error Estimation for discontinuous Galerkin Methods for Convection Diffusion Problems, University of British Columbia, 2010 Ph.D. thesis. URL <https://open.library.ubc.ca/cIRcle/collections/24/items/4661.0069593>
- [29] P. Solin, K. Segeth, I. Dolezel, *Higher-Order Finite Element Methods*, CRC Press, 2003.
- [30] N. Heuer, M.E. Mellado, E.P. Stephan, hp -adaptive two-level methods for boundary integral equations on curves, *Computing* 67 (4) (2001) 305–334.
- [31] T. Eibner, J.M. Melenk, An adaptive strategy for hp -FEM based on testing for analyticity, *Comput. Mech.* 39 (5) (2007) 575–595.
- [32] P. Houston, E. Süli, A note on the design of hp -adaptive finite element methods for elliptic partial differential equations, *Comput. Methods Appl. Mech. Eng.* 194 (2) (2005) 229–243.
- [33] P. Houston, B. Senior, E. Süli, Sobolev regularity estimation for hp -adaptive finite element methods, in: F. Brezzi, A. Buffa, S. Corsaro, A. Muri (Eds.), *Numerical Mathematics and Advanced Applications*, Springer, Milano, 2003, pp. 631–656.
- [34] B. Guo, I. Babuška, The hp version of the finite element method, *Comput. Mech.* 1 (1) (1986) 21–41.
- [35] S. Giani, E.J. Hall, An a posteriori error estimator for hp -adaptive discontinuous Galerkin methods for elliptic eigenvalue problems, *Mathem. Models Methods Appl. Sci.* 22 (10) (2012) 1250030.
- [36] G.R. Irwin, Analysis of Stresses and Strains Near the End of a Crack Traversing a Plate, *SPIE Milestone Series MS*, 137, 1997, p. 16.